南京信息工程大学
Nanjing University of Information Science & Technology

Opposite trends of NH and SH monsoon in the past century

Jian Cao

Nuist

Co-authors：Hao Wang, Haikun Zhao, Chao Wang(NUIST, CHINA)
B. Wang (Hawaii University, USA)
Xiaowei Zhu (Ningxia Climate Center, CHINA)

- Cao, J., H. Wang, B. Wang, H. Zhao C. Wan. X. Zhu, 2021: Higher Sensitivity of Northern Hemisphere Monsoon to Anthropogenic Aerosol Than Greenhouse Gases. Geophysical Research Letters, 49, e2022GL100270.
- Cao, J., X. Lian, M. Cao, B. Wang, X. Zhu, H. Zhao, 2023: Wettening of Southern Hemisphere land monsoon during 1901-2014. Journal of Climate. 36, 8497-8512.

南京信息工程大学
Nanjing University of Information Science & Technology

Outline

- Part 1- Introduction
- Part 2- Data and methods
- Part 3- External forcing drive long-term NH monsoon change
- Part 4- Tropical SST gradient forced SH monsoon increase
- Part 5- Summary

Part 1：Global monsoon

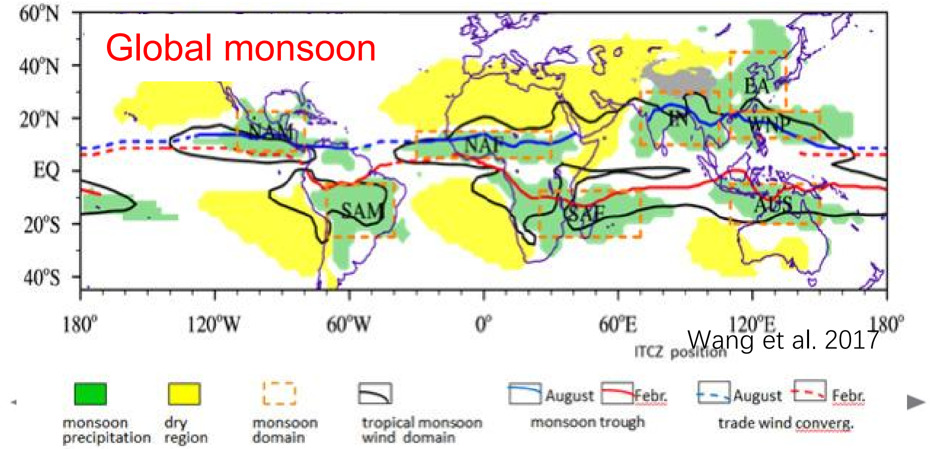

Wang et al. 2017

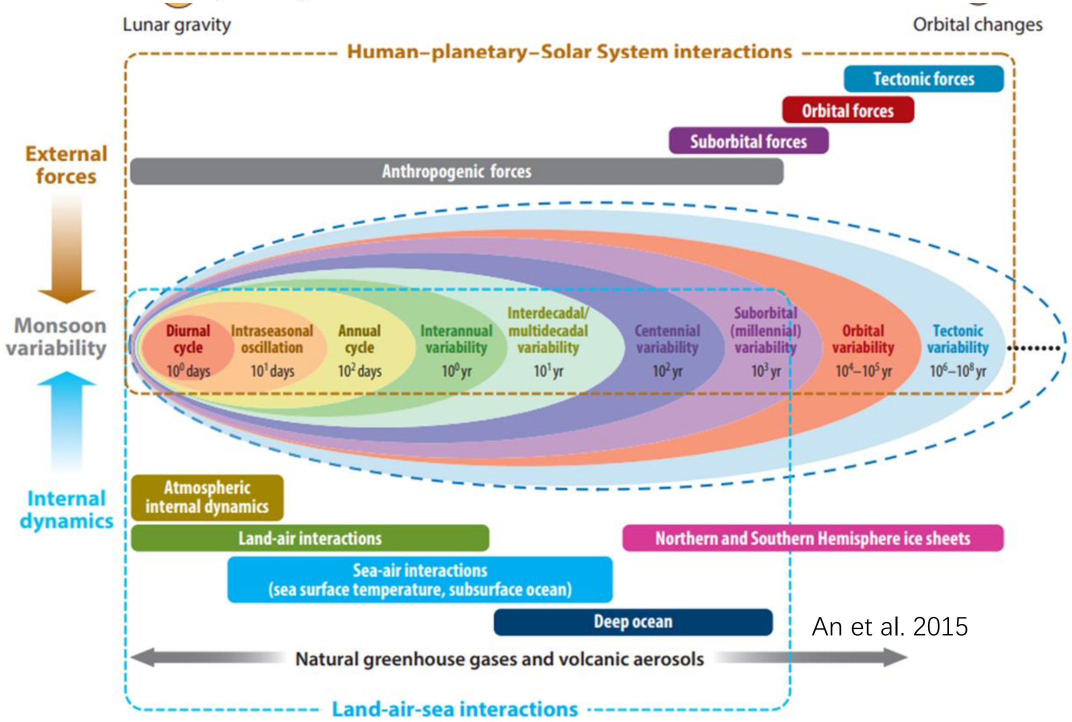

An et al. 2015

Global mean surface air temperature

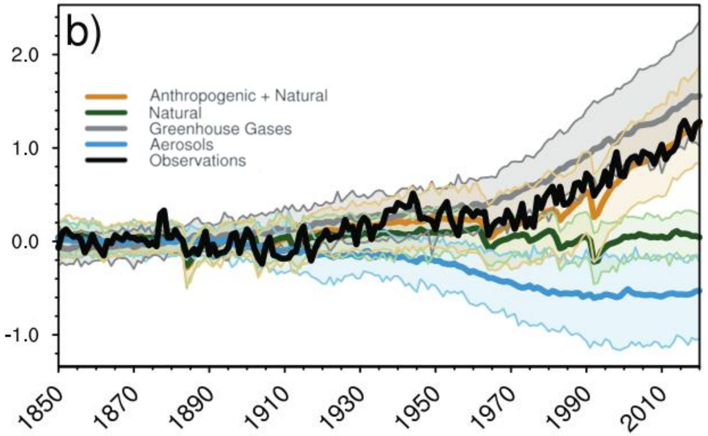

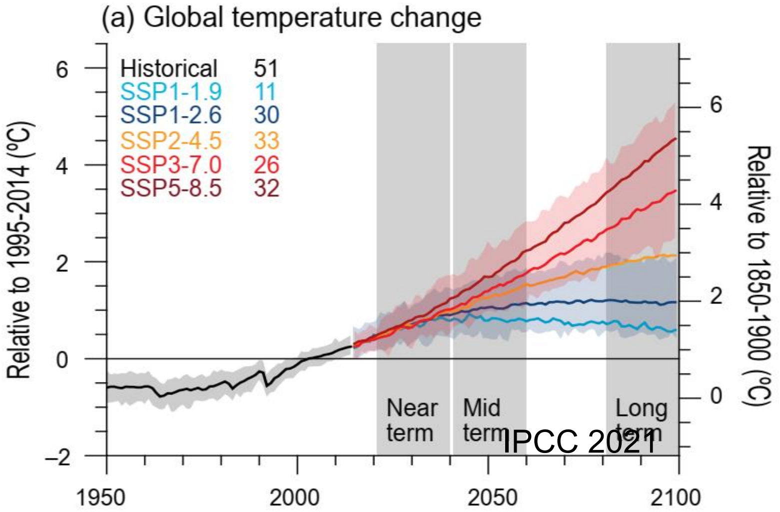

IPCC 2021

Figure 4.2 | Selected indicators of global climate change from CMIP6 historical and scenario simulations.

Part 1：NH monsoon vs. SH monsoon

南京信息工程大学
Nanjing University of Information Science & Technology

Past 21K： Anti-phase relationship between NH and SH monsoon precipitation due to ice melting

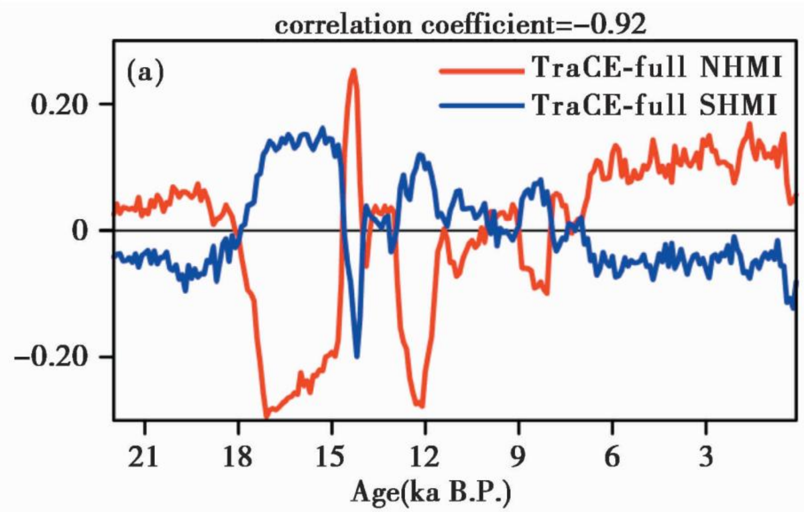

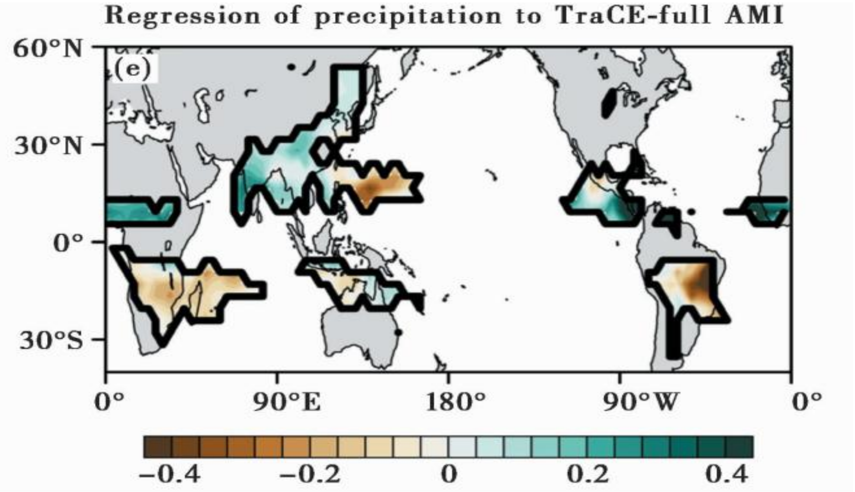

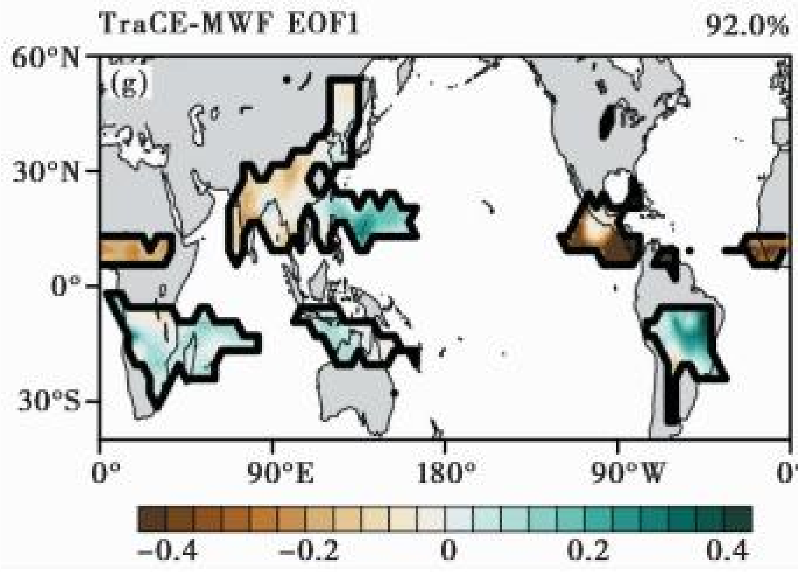

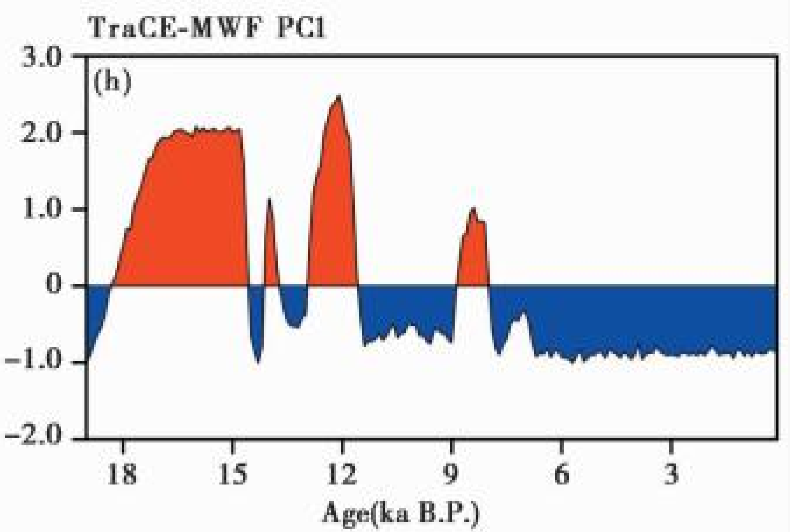

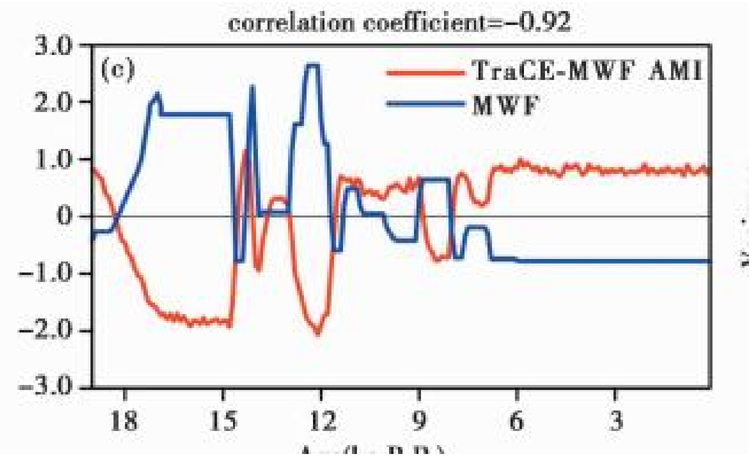

Li et al., 2022

Part 1：NH monsoon vs. SH monsoon

南京信息工程大学
Nanjing University of Information Science & Technology

Past 1K: Role of GMST

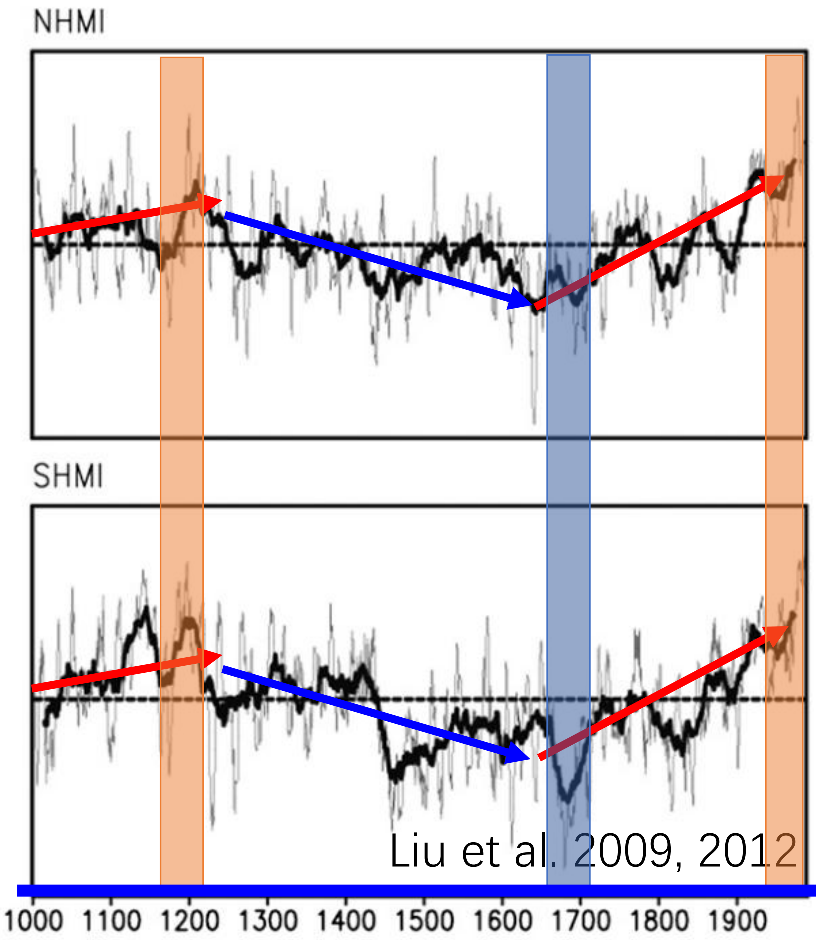

?

Future one century
NH: Thermal Contrast
SH: ???

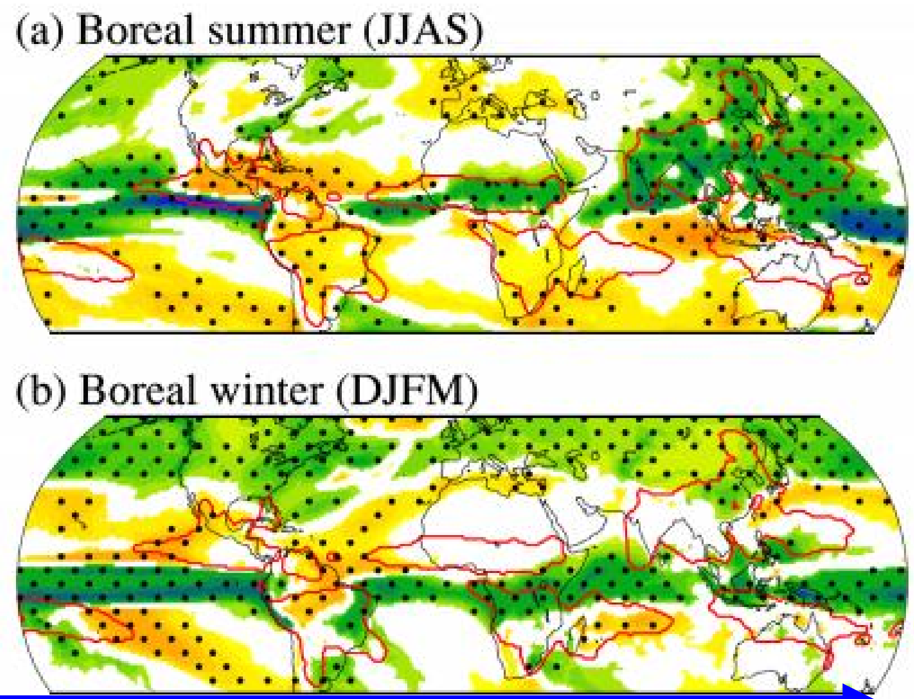

Wang et al. 2020

1000 1900 2000 2100

Part 1： Global Warming and Monsoons

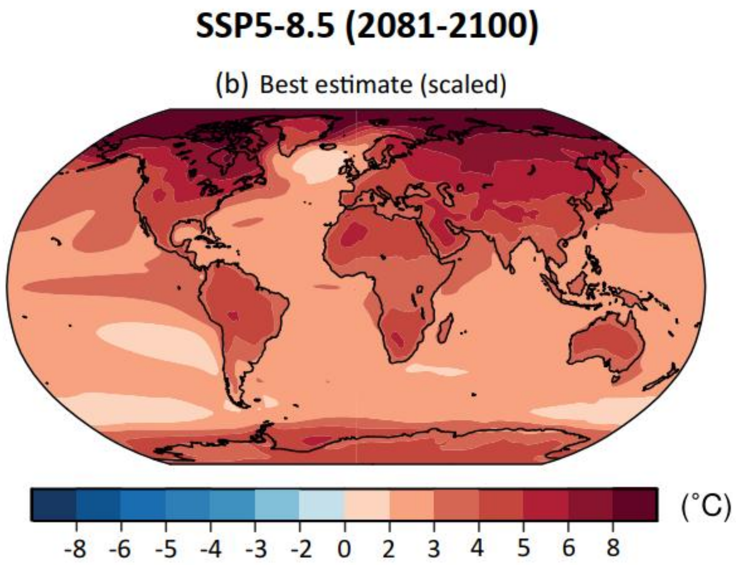

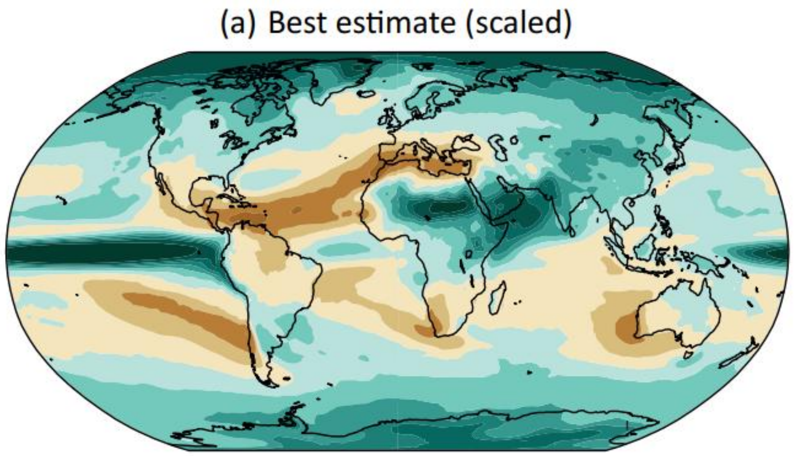

Figure 4.41 | High-warming storylines for changes in annual mean temperature.

Figure 4.42 | High-warming storylines for changes in annual mean precipitation.

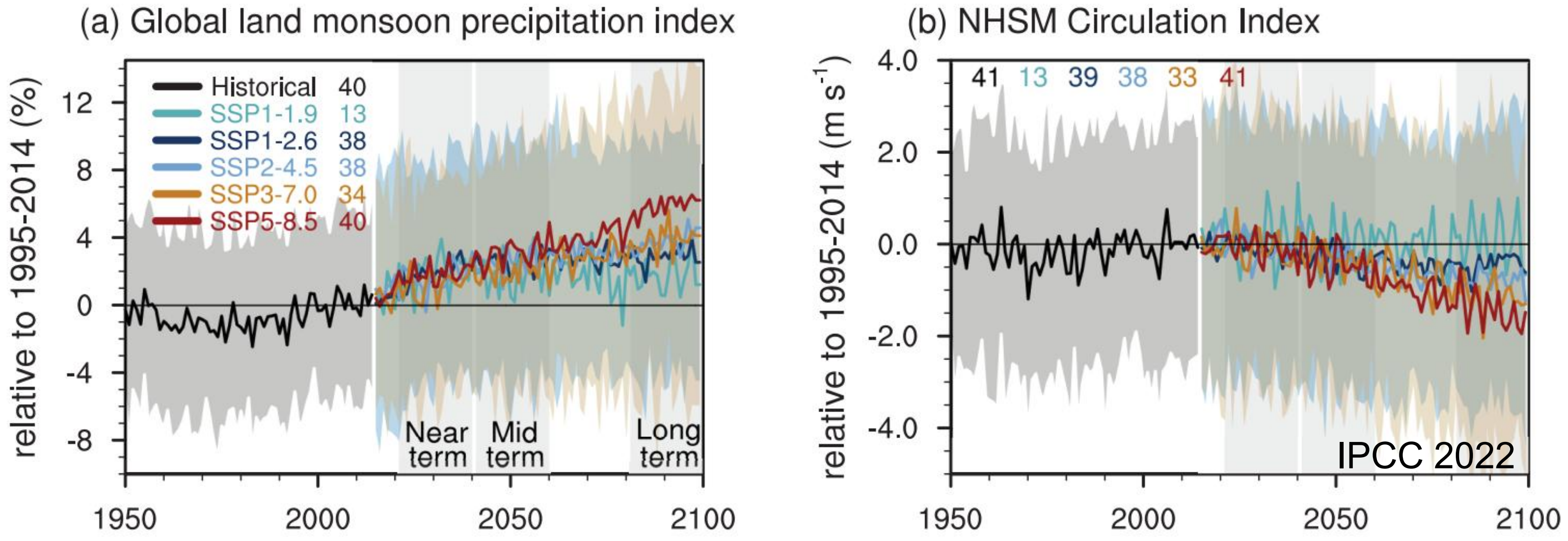

Figure 4.14 | Time series of global land monsoon precipitation and Northern Hemisphere summer monsoon (NHSM) circulation index anomalies

Part 1: Changes in NH Monsoon

南京信息工程大学
Nanjing University of Information Science & Technology

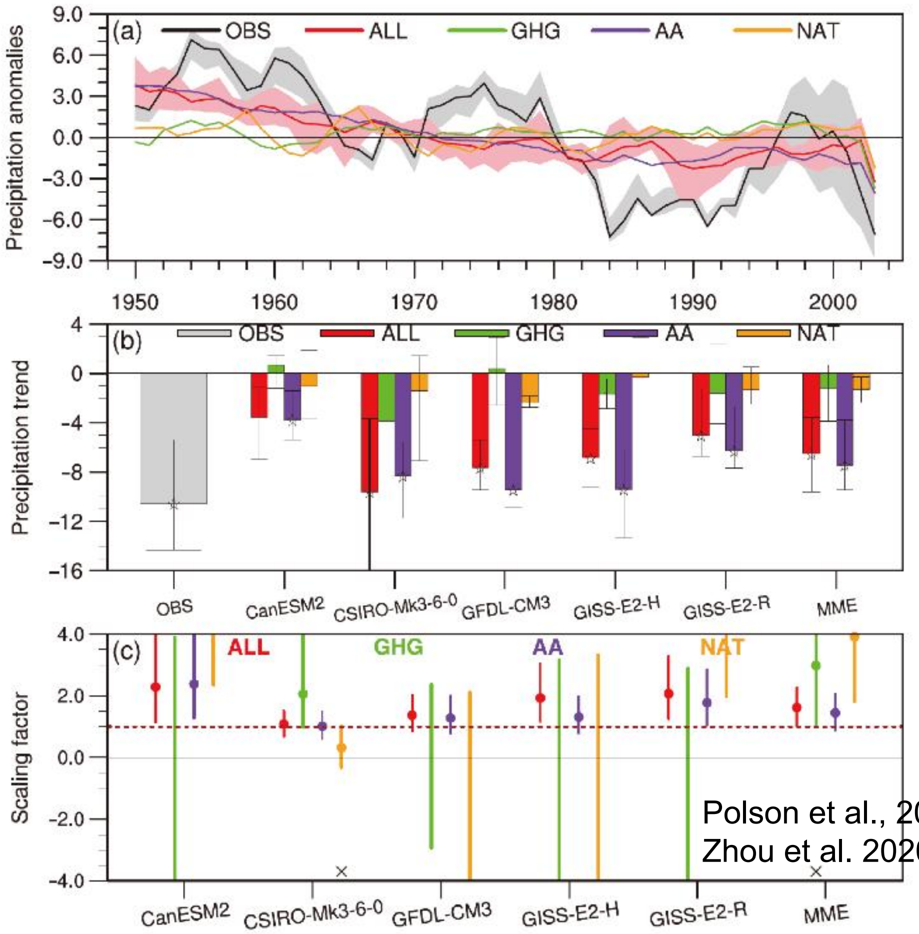

Polson et al., 2014
Zhou et al. 2020

Detection and attribution of global land monsoon precipitation changes under different forcing agents. (a) global land monsoon precipitation anomalies. Linear trends in global land monsoon precipitation. (c) The results of the optimal fingerprinting detection.

Part 1： Global Warming and Monsoons

Nanjing University of Information Science & Technology

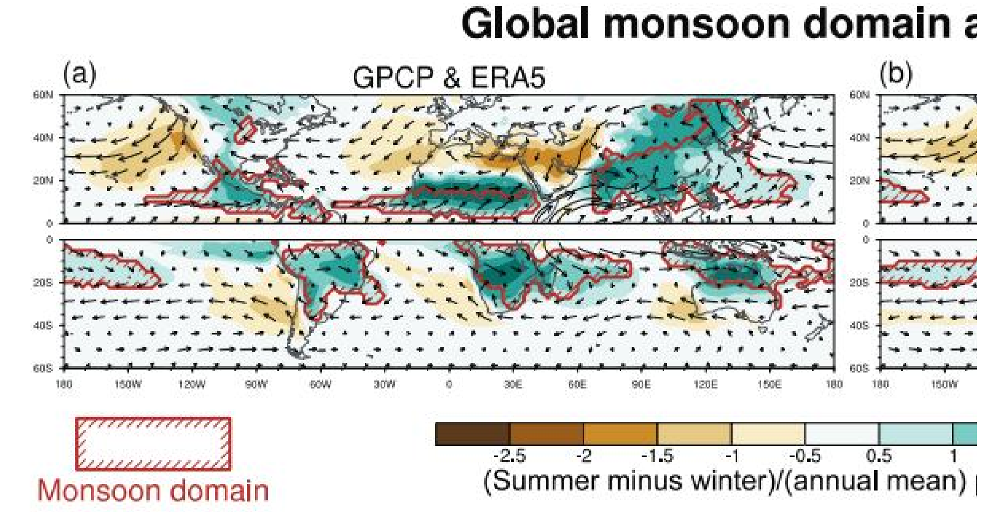

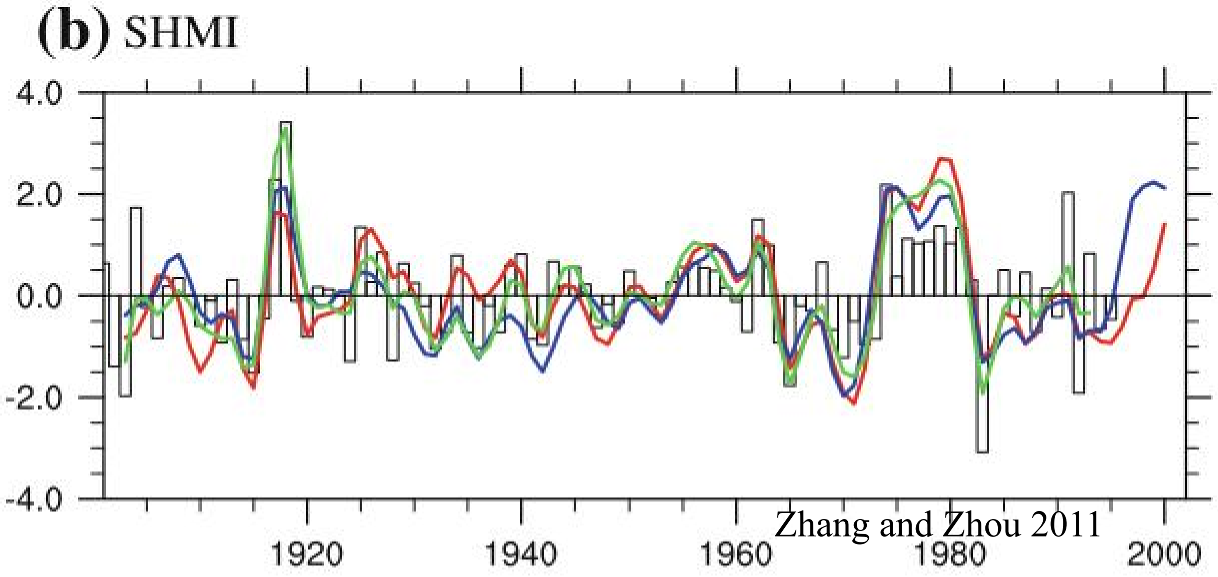

Zhang and Zhou 2011

ı of global
ıd

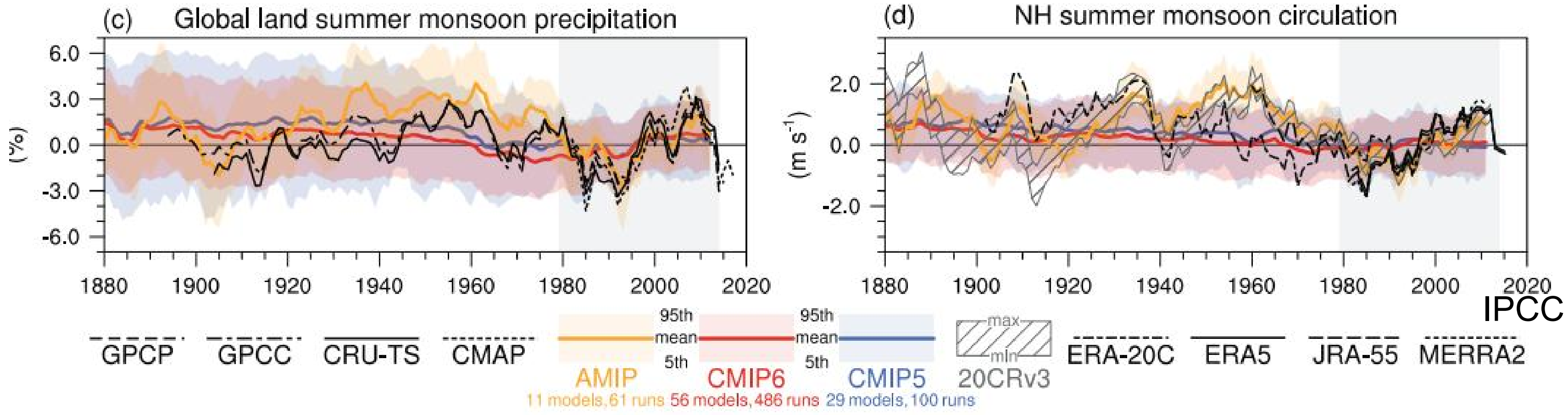

IPCC 2022

Questions？

- Why is NH monsoon precipiation weakened since 1900s, but the SH monsoon rainfall increased?

- Why does the AA forcing dominate the declining NHLM precipitation, although AA's impacts on Earth system radiative forcing and GMST are less than GHG?

- Which mechanism is responsible for the increase of SH monsoon?

Part 2: Model data and Method

Var	Source	Usage
Surface temperature	HadCRUT4	
Precipitation	Global Precipitation Climatology Centre (GPCC), Version 7 Climate Research Unit (CRU), Version 4.04 the University of Delaware (UDel), Version 4.01	Examine the long-term change in monsoon precipitation
	Global Precipitation Climatology Project (GPCP)	Define the monsoon domain

Monsoon domain is defined where the precipitation difference between summer (May-September, MJJAS) and winter (November-March) exceeds 2.5 mm/d, and summer precipitation accounts for at least 55% of the annual total.

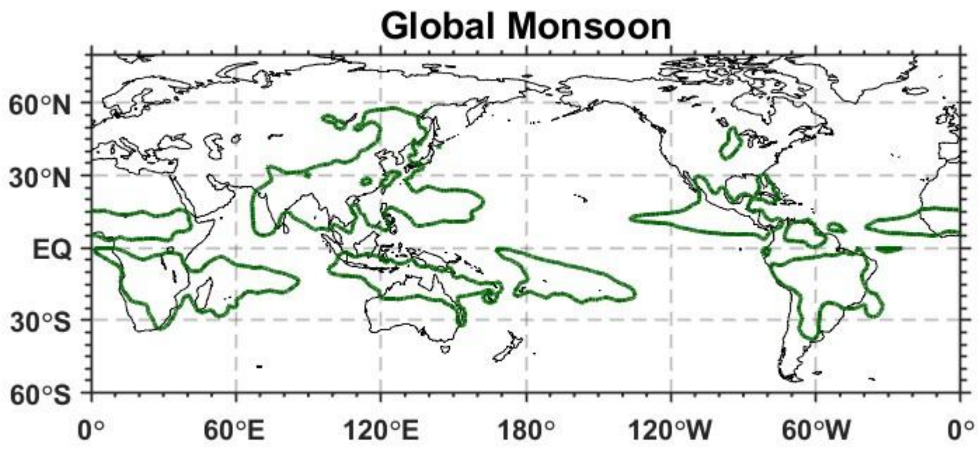

Part 2: Model data and Method

南京信息工程大学
Nanjing University of Information Science & Technology

CMIP6 models description

Model name	Atmosphere resolution	Model name	Atmosphere resolution
ACCESS-CM2	192x144	CESM2-WACCM	288x192
ACCESS-ESM1-5	192x145	E3SM-1-0	360x180
BCC-CSM2-MR	320x160	E3SM-1-1	360x180
CESM2	288x192	EC-Earth3-Veg	512x256
CNRM-CM6-1	256x128	EC-Earth3	512x256
CanESM5	128x64	FGOALS-f3-L	288x180
FGOALS-g3	180x80	FIO-ESM-2-0	288x192
GFDL-ESM4	288x180	GISS-E2-1-G-CC	144x90
GISS-E2-1-G	144x90	GISS-E2-1-H	144x90
HadGEM3-GC31-LL	192x144	IITM-ESM	192x94
IPSL-CM6A-LR	144x143	INM-CM4-8	180x120
MIROC6	256x128	INM-CM5-0	180x120
MRI-ESM2-0	320x160	MCM-UA-1-0	96x80
NorESM2-LM	144x96	MIROC-ES2L	128x64
AWI-ESM-1-1-LR	192x96	MPI-ESM1-2-HR	384x192
BCC-ESM1	128x64	MPI-ESM1-2-LR	192x96
CAMS-CSM1-0	320x160	NESM3	192x96
CESM2-FV2	144x96	NorCPM1	144x96
CESM2-WACCM-FV2	144x96	SAM0-UNICON	288x192

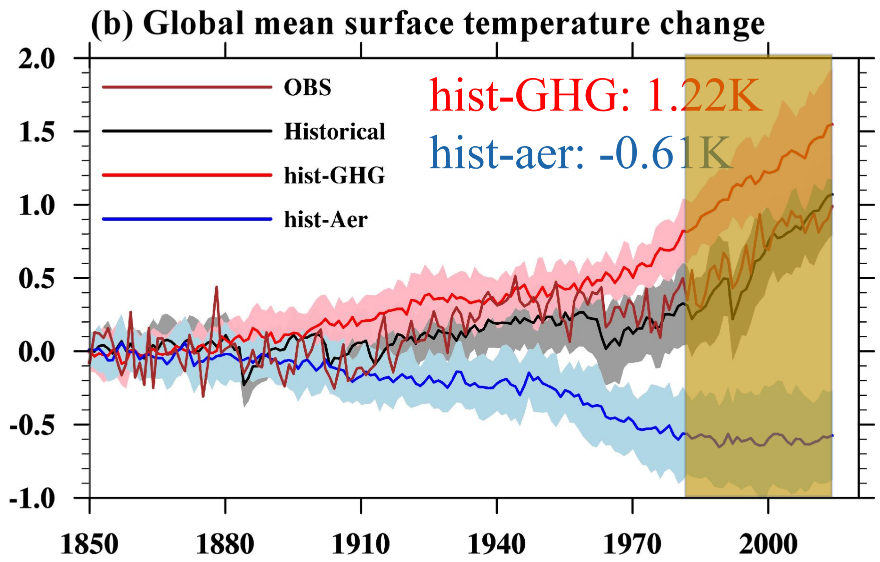

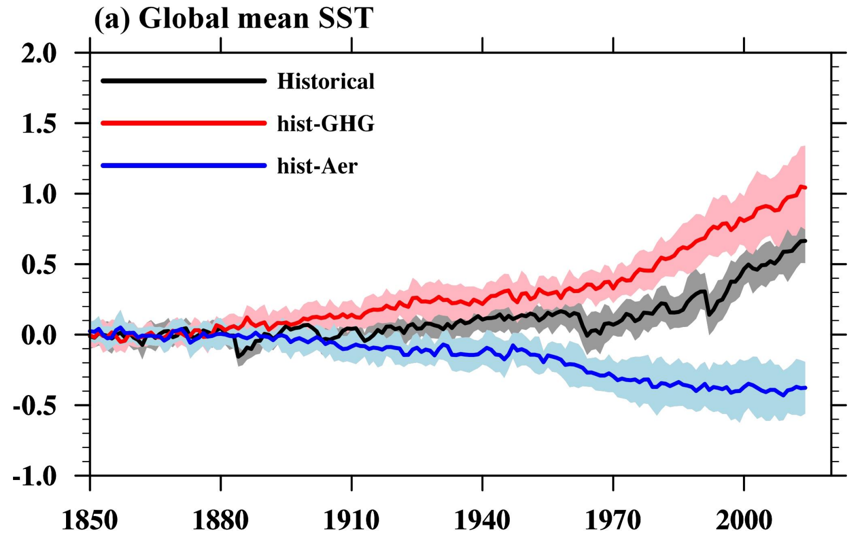

Part 3: NH monsoon change

Nanjing University of Information Science & Technology

Linear trends of Observed and simulation NHLM precipitation

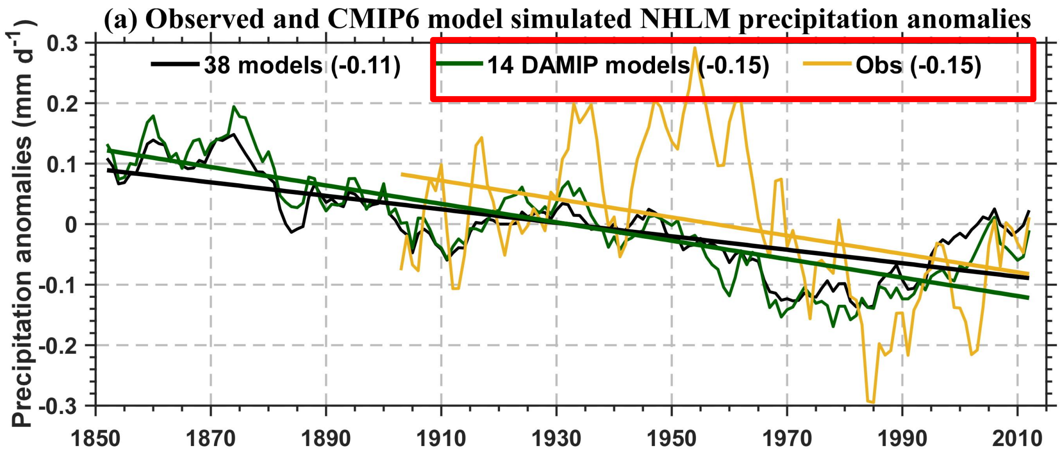

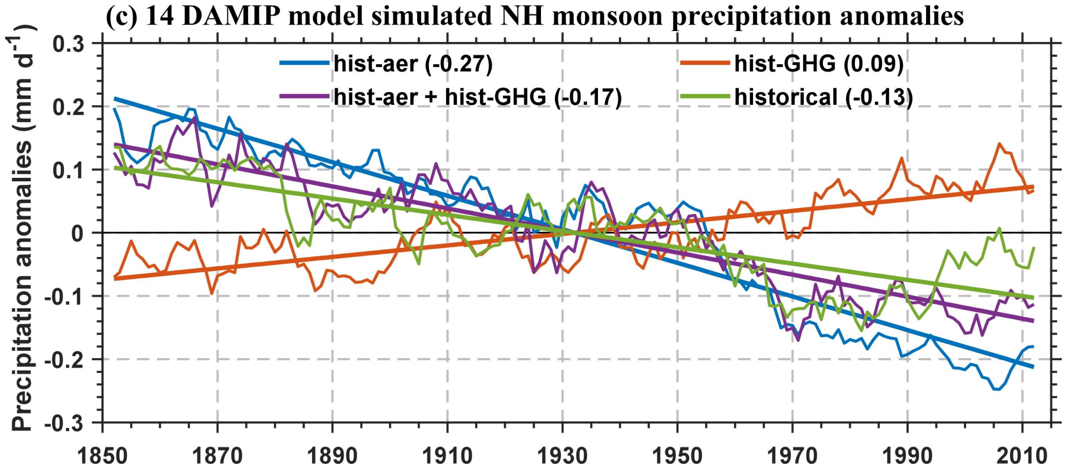

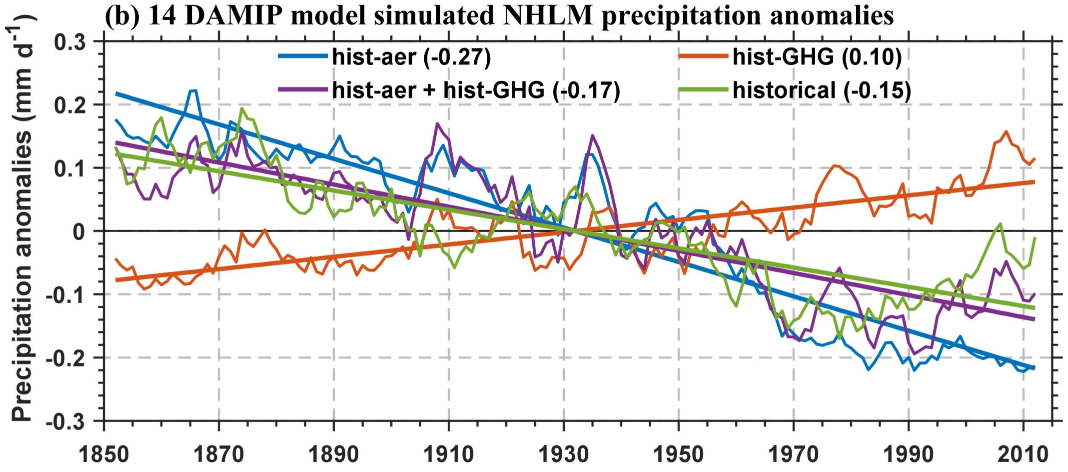

	Trend (mm/d/cent)
OBS	-0.15
Historical	-0.15(DAMIP),-0.11(All)
GHG	+0.10
AA	-0.27

Part 3: NH monsoon change

Higher Sensitivity of NHLM to AA than GHG

(a) Land monsoon pre. anomalies versus GMST changes

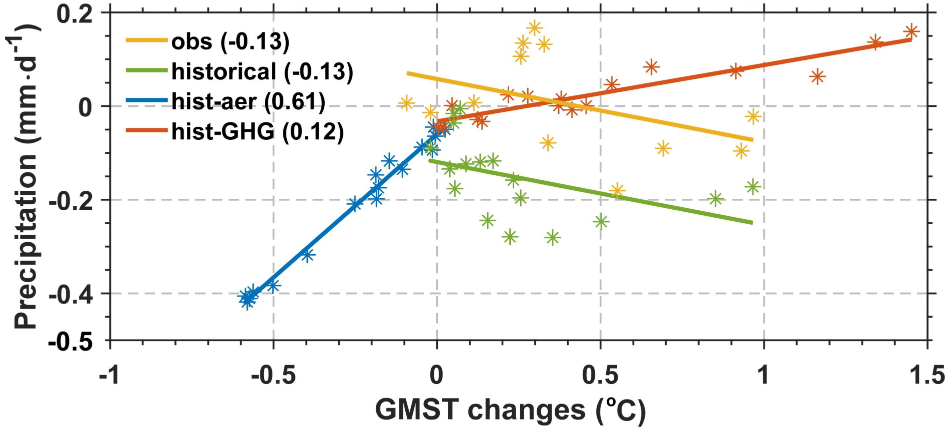

Scatter plots of decadal means of the precipitation anomalies versus GMST changes

(b) Moisture budget per Kelvin

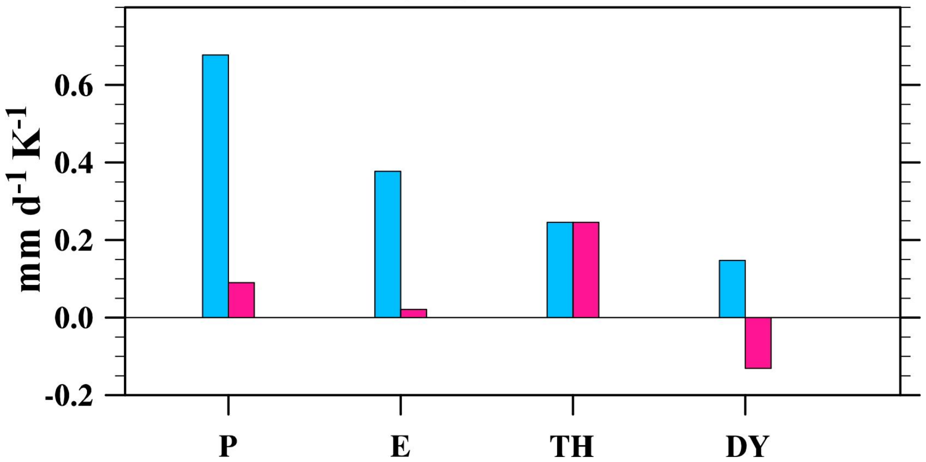

Top of Atmosphere (TOA) radiative forcing (W m^{-2})

Model name	aerosols RF	GHG RF
MME	-1.14	2.94

Moisture budget analysis:

$$P' \approx E' - \langle \overline{\omega} \partial_p q' \rangle - \langle \omega' \partial_p \overline{q} \rangle$$

GHG: TH (+), DY (-) Cancelation

AA: E* (+), TH (+), DY* (+) Amplification

~11%/K for AA v.s. ~2.2%/K for GHG

Part 3: Results

南京信息工程大学
Nanjing University of Information Science & Technology

Surface energy change explains the evaporation term

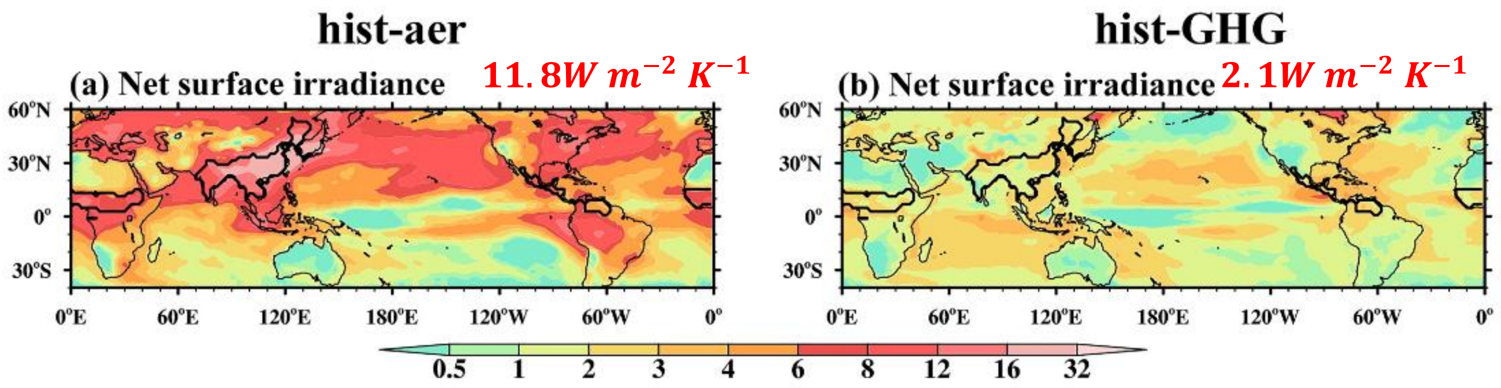

In monsoon region, the surface evaporation is more constrained by the available energy for evaporation (Liepert et al., 2004; Roderick et al., 2014).

$$E = \frac{mR_n + \rho_a c_p (\delta_e) g_a}{\lambda_v (m+\gamma)}$$

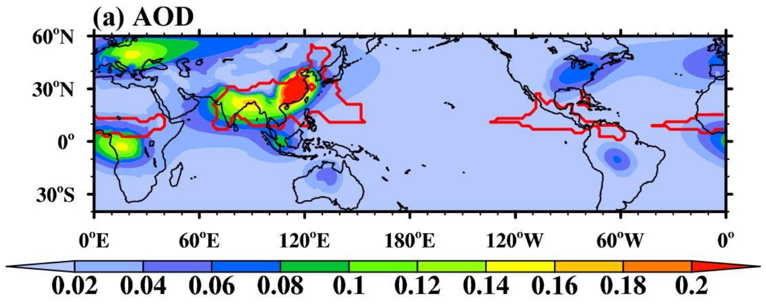

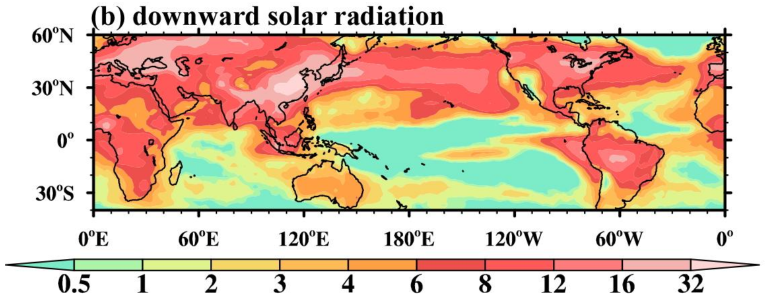

The upper row shows net surface irradiance,
the middle row shows downward solar radiation,
and the bottom row shows the aerosol optical depth

R_n more important

↑

downward solar radiation

↑

aerosol-radiation & aerosol-cloud interactions

Part 3: NH monsoon change

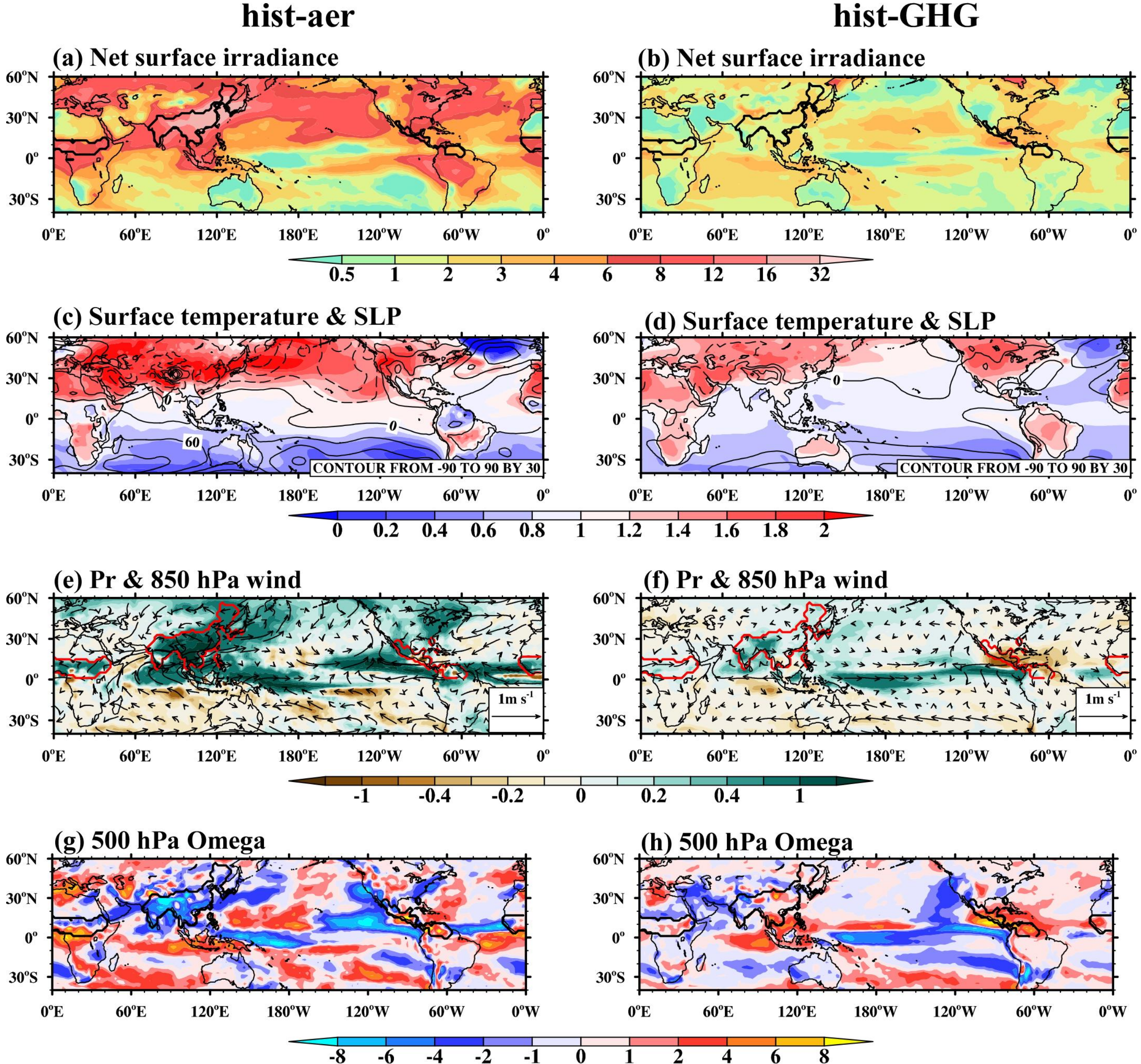

Comparison of atmospheric variables responds to anthropogenic aerosol (AA) (left) and greenhouse gases (GHG) (right) forcing. All changes are scaled by the corresponding global mean surface temperature (GMST) changes from hist-aer and hist-GHG experiments. (a and b) for net surface irradiance (W m^{-2} K^{-1}). (c and d) for surface temperature (shading, K K^{-1}) and sea level pressure (contour, Pa K^{-1}). (e and f) for precipitation (mm d^{-1} K^{-1}) and 850 hPa circulation (m s^{-1} K^{-1}). (g) and (h) for vertical pressure velocity (hPa d^{-1} K^{-1}) at 500 hPa. The black and red lines outline the Northern Hemisphere (NH) land monsoon region

Part 3: NH monsoon change

南京信息工程大学
Nanjing University of Information Science & Technology

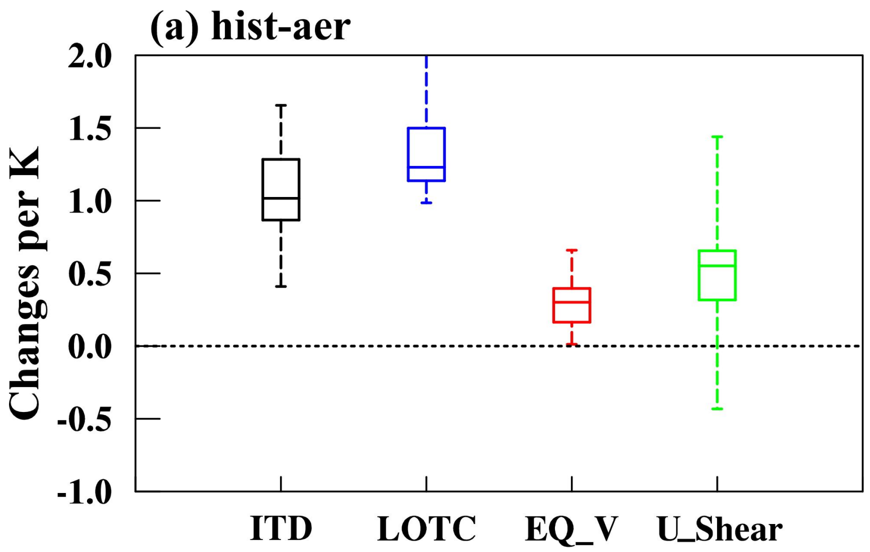

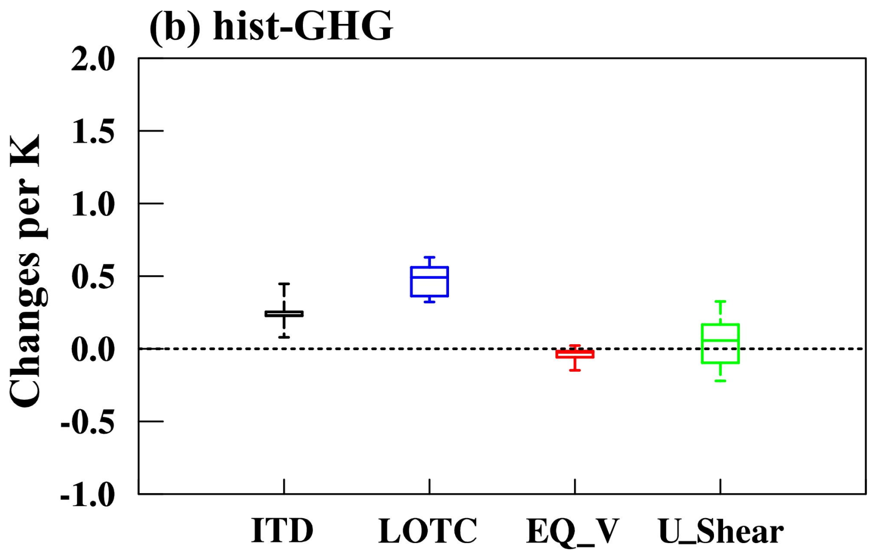

ITD index: the surface temperature difference between the NH [0–40°N, 0°–360°] and SH [0°–60°S, 0°–360°].

LOTC index: the temperature difference between NH land [0°–60°N, 0°–360°] and global ocean [60°S–60°N, 0°–360°].

EQ_V index (the low-level cross-equatorial flow from the SH to NH): the meridional wind averaged over [5°S–10°N, 0°–360°] at 925 hPa.

U_shear index: the zonal wind shear between 200 and 850 hPa over the band of [0°–20°N, 120°W–120°E]

Increase aerosol weakens monsoon circulation

ITD weaker

↓

high pres in NH
low pres in SH

↓

southward flow

LOTC weaker

↓

zonal wind shear weaker

↓

weaken the moisture convergence

南京信息工程大学
Nanjing University of Information Science & Technology

Outline

- Part 1- Introduction
- Part 2- Model and method
- Part 3- External forcing drive long-term NH monsoon change
- Part 4- Tropical SST gradient forced SH monsoon increase
- Part 5- Summary

Part 4: SH monsoon change

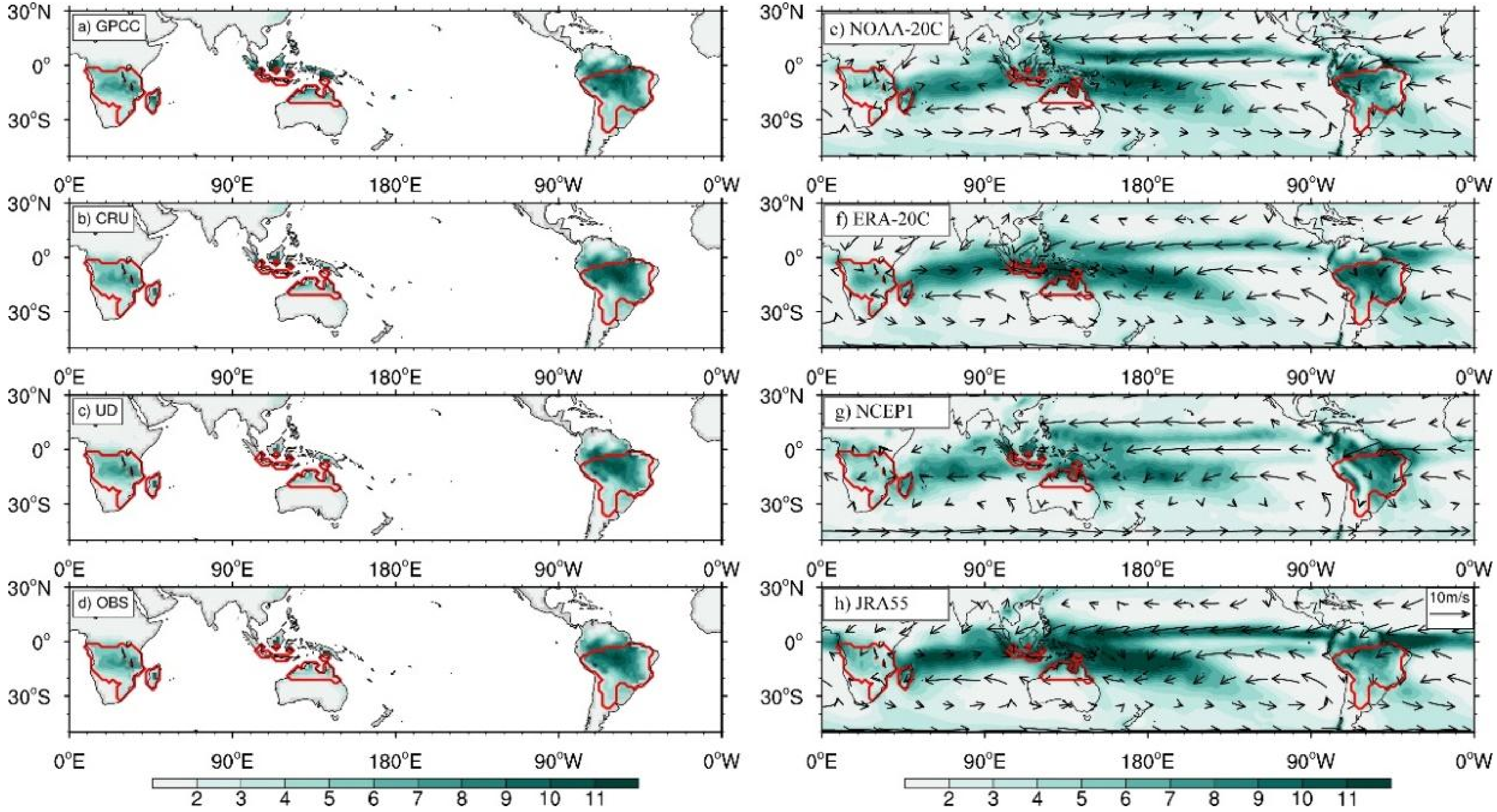

Figure 1 Climatology of boreal winter (DJFM) precipitation (mm d^{-1}) and 850 hPa circulation (m s^{-1}) for the period of 1985-2014. The observation and reanalysis are shown in the left and right panel, respectively. (a) GPCC, (b) CRU, (c) UD, (d) the average of (a-c) as OBS, (e) NOAA-20C, (f) ERA-20C, (g) NCEP1, and (h) JRA55. The red curves outline the SHLM region.

Part 4: Wettenning of SHLM

南京信息工程大学
Nanjing University of Information Science & Technology

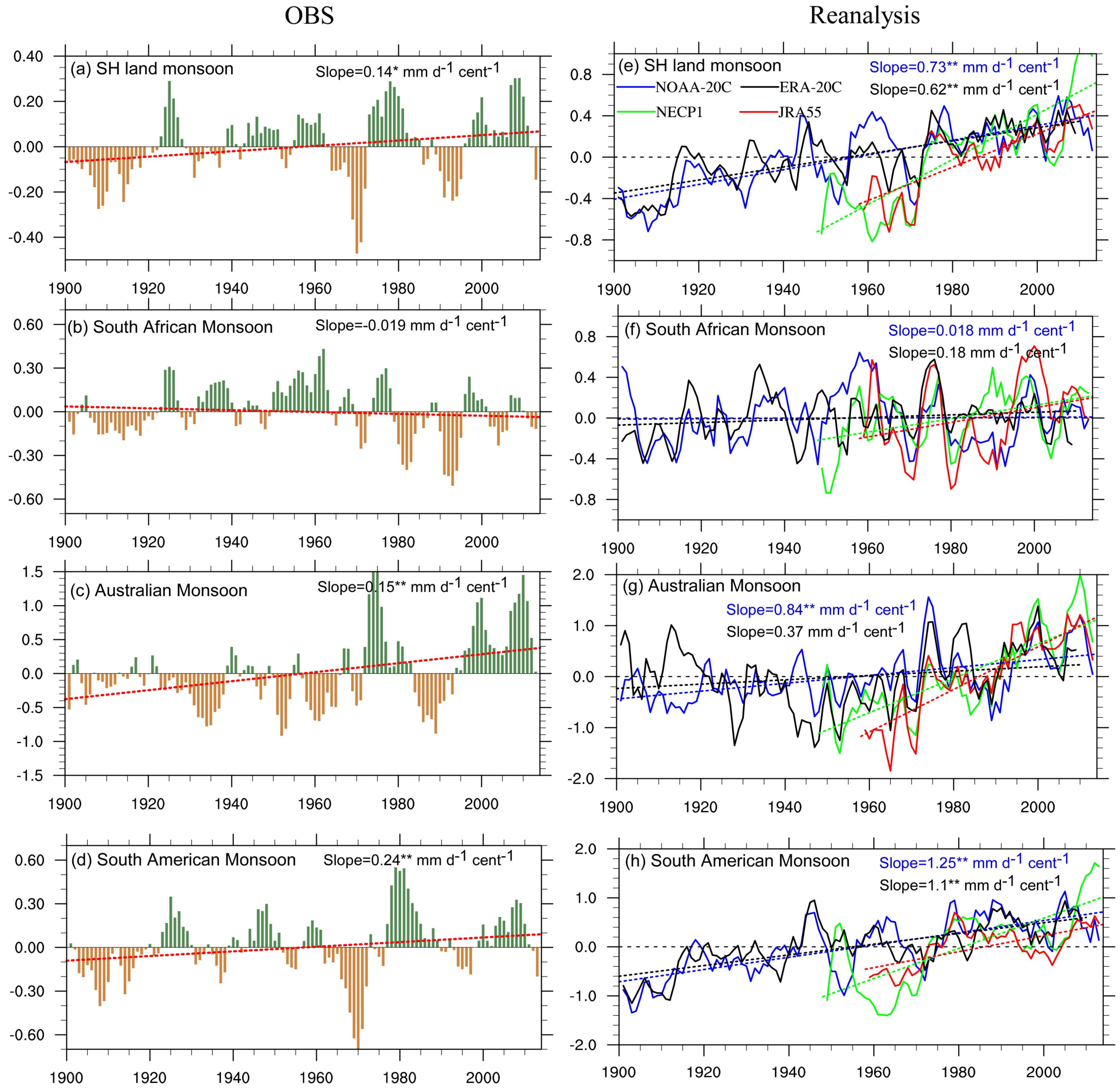

Table 2 Linear trends (mm d^{-1} $cent^{-1}$) of SHLMP in observation and reanalysis. * and ** indicate the significance of 95% and 99%.

Region	OBS	NOAA-20C	ERA-20C
SH monsoon	0.14*	0.73**	0.62**
SAF	0.083	0.029	0.18
AUS	0.15**	0.84**	0.37
SAM	0.24**	1.25**	1.1**

Changes of SHLM and three regional monsoon precipitation (mm d^{-1}) from observation (left) and four reanalysis datasets (right). (a, e) for SHLMP, (b,f) for SAF precipitation, (c, g) for AUS precipitation, and lower panel (d, h) for SAM precipitation. The bars in (a) and solid curves in (b) indicate the 3-year running mean SHLMP. The dashed lines indicate linear trends.

Part 4: Wettenning of SHLM

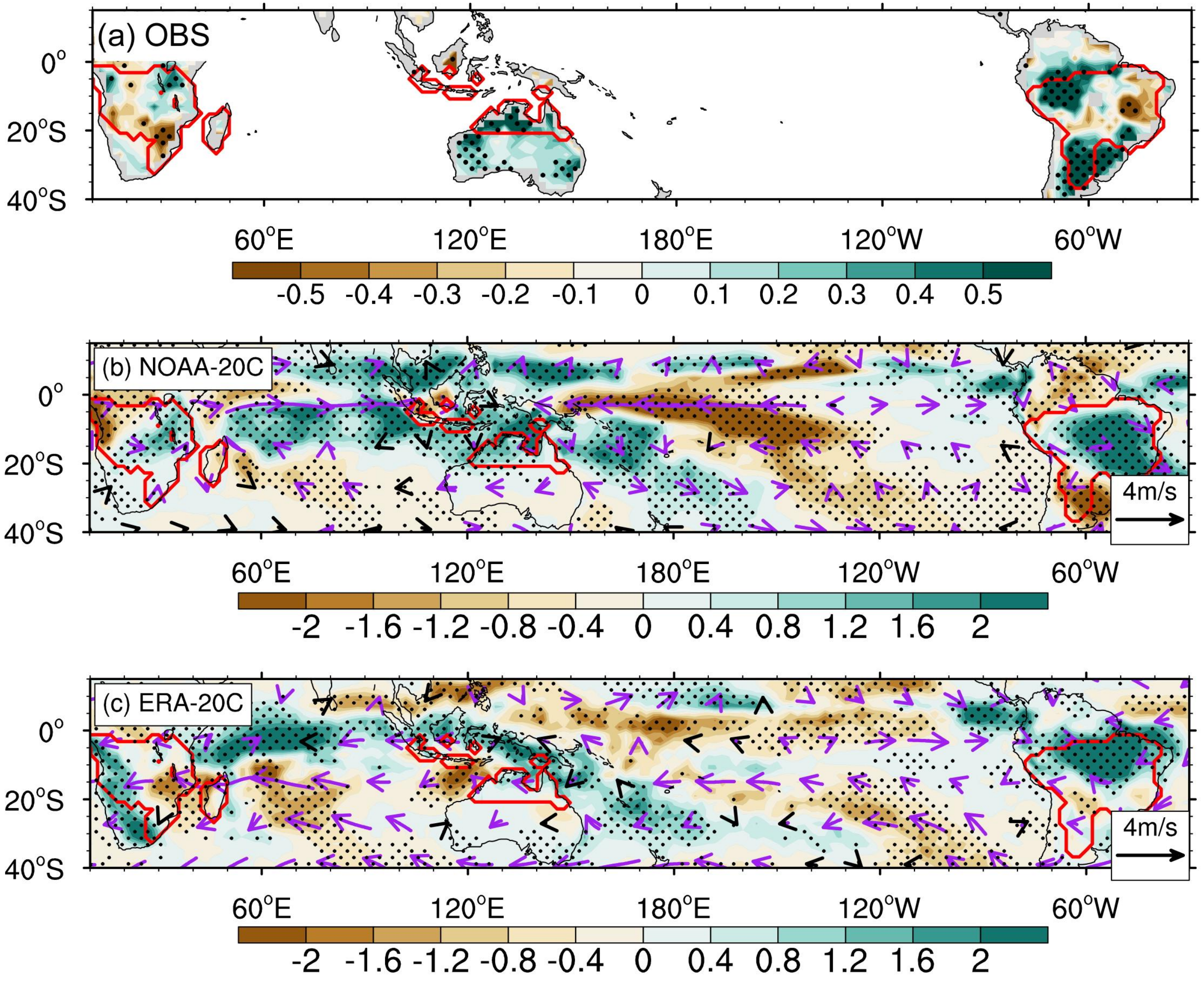

Linear trends of precipitation (mm d^{-1} $cent^{-1}$) and 850 hPa circulation (m s^{-1} $cent^{-1}$) during austral summer (DJFM) for observation (left) and reanalysis (right). (a) for GPCC during 1901-2014, (b) for CRU during 1901-2014, (c) for UD during 1901-2014, (d) for OBS (the average of GPCC, CRU, and UD) during 1901-2014. (e) for NOAA-20C during 1901-2014. (f) for ERA-20C during 1901-2010, (g) for NECP1 during 1949-2014, and (h) for JRA55 during 1959-2014. The red curves outline the SHLM region.

南京信息工程大学
Nanjing University of Information Science & Technology

Part 4: Mechanism

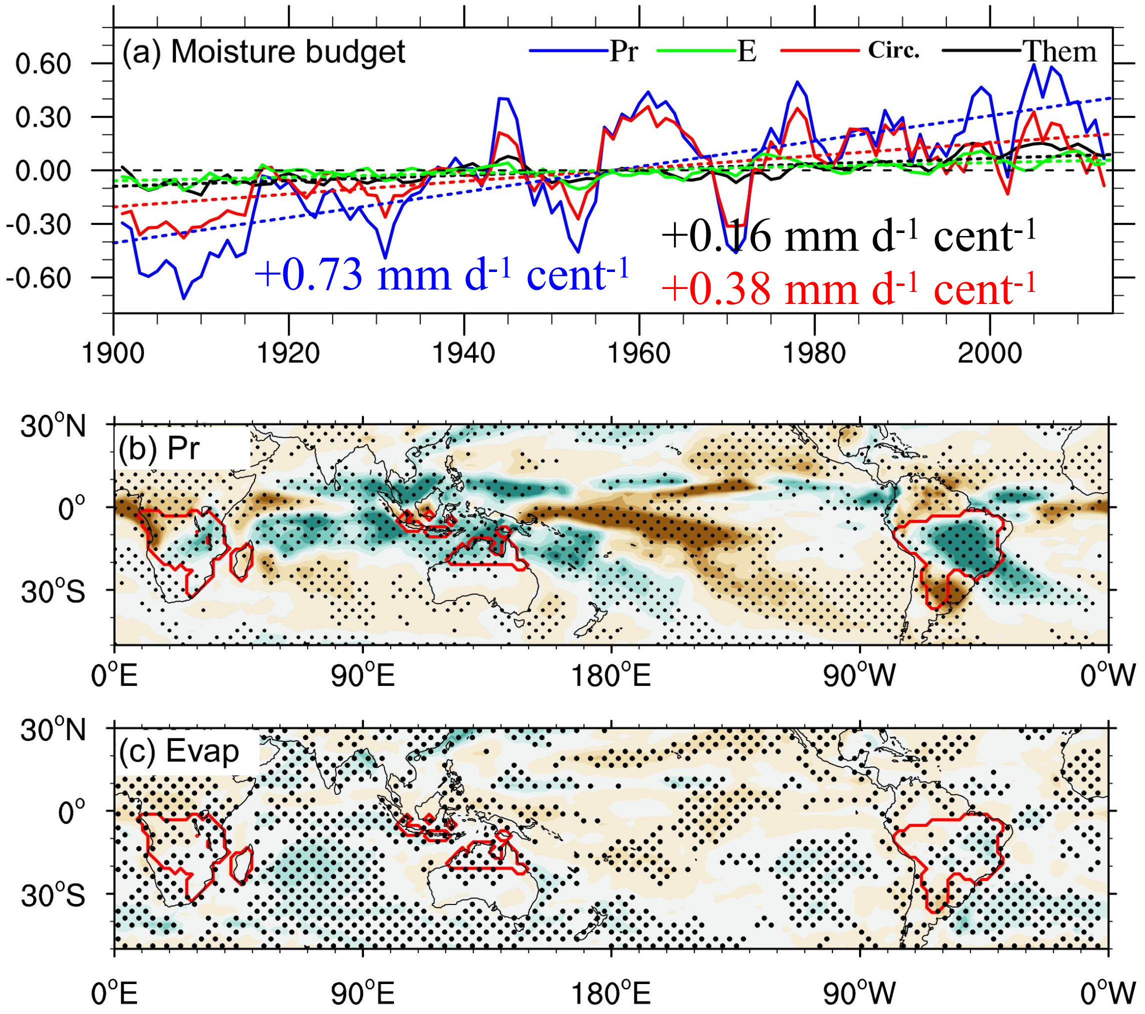

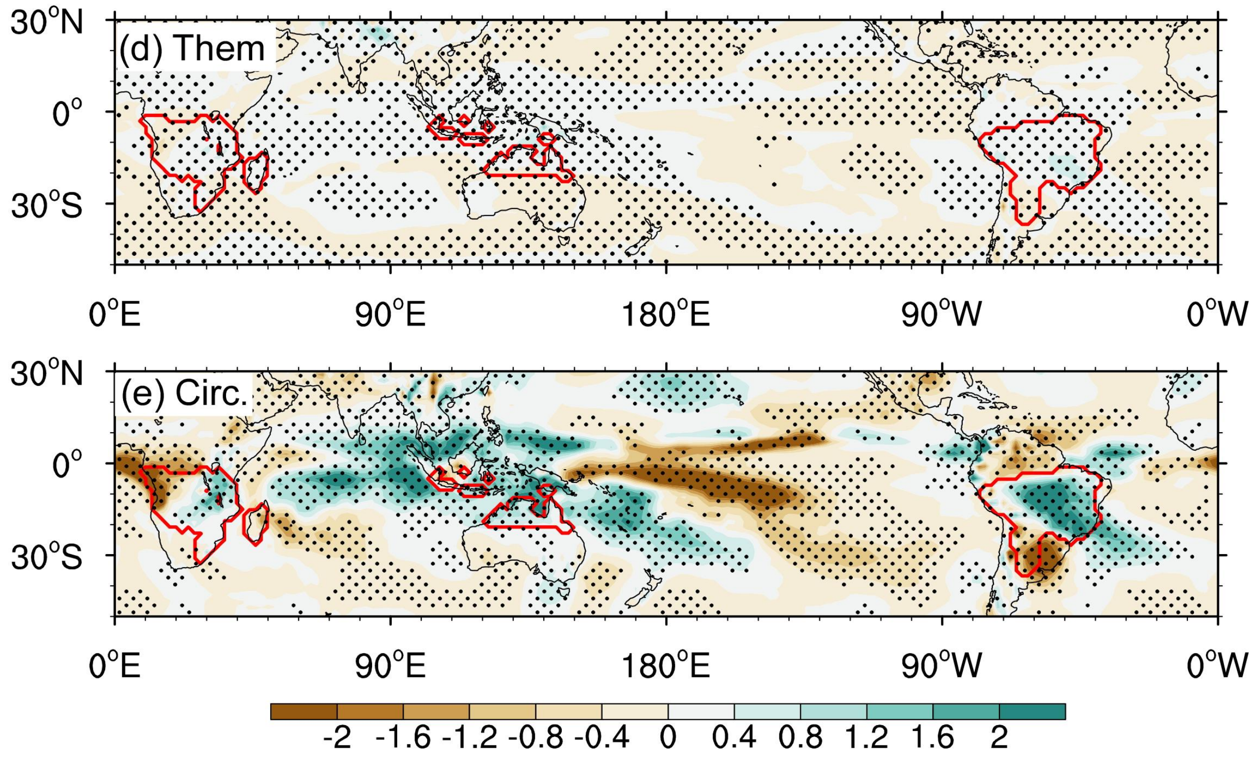

Moisture budget analysis for the SHLMP change. (a) Moisture budget terms over the SHLM region (mm d^{-1}). Linear trends (mm d^{-1} $cent^{-1}$) for (b) precipitation, (c) evaporation, (d) Moisture term, and (e) Circulation term.

Part 3: Mechanism

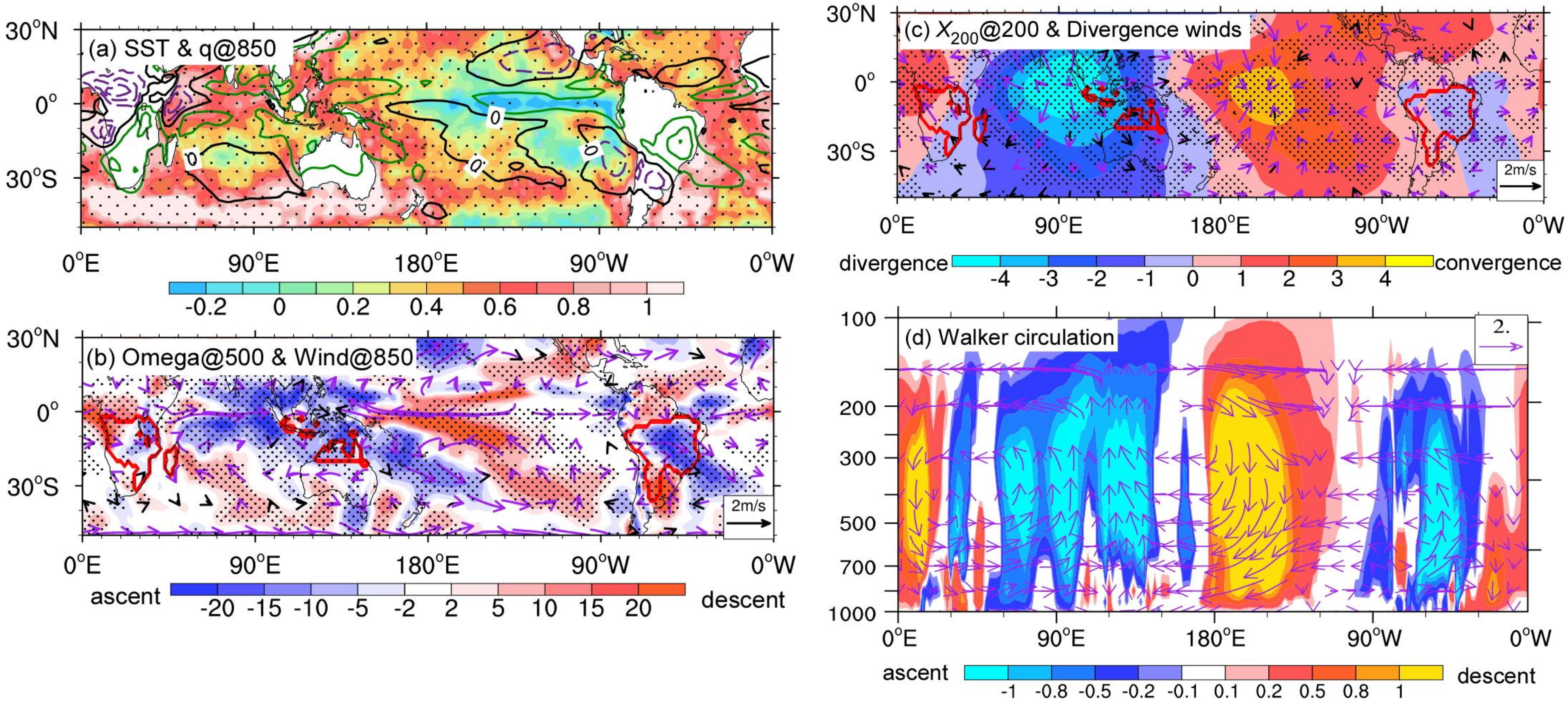

(a) Linear trends of SST (shading, K cent^{-1}) and 850 hPa specific humidity (contours, g kg^{-1} cent^{-1}). (b) Linear trends of 500 hPa vertical pressure velocity (shading, 100*omega, Pa s^{-1} cent^{-1}) and 850 hPa circulation (vectors, m s^{-1} cent^{-1}). (c) Linear trends of velocity potential (shading, 10^6 m^2 s^{-1} cent^{-1}) and divergence winds (vectors, m s^{-1} cent^{-1}). The purple and green lines indicate the positive and nagtive trends of 850 hPa specific humidity, respectively, with the zero line ploting in black.

Part 3: Monsoon circulation indices

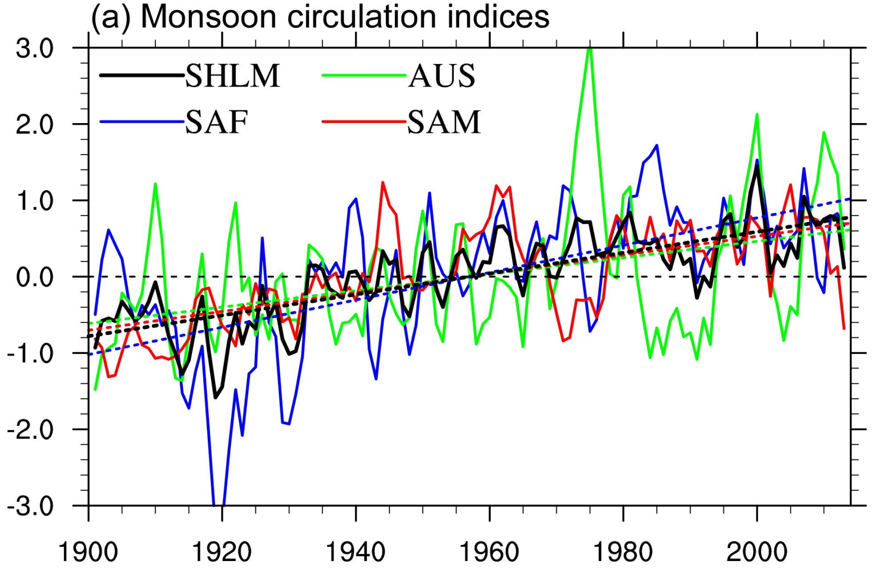

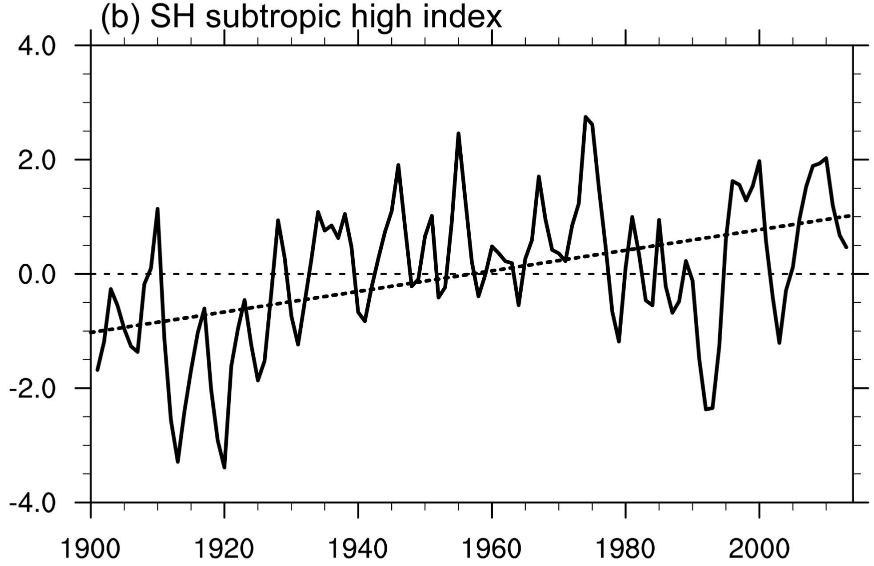

Region	Definition of the circulation index
NAF	U850 (0°–15°N, 30°W–30°E)
SA	U850 (10°–20°N, 40°–80°E) minus U850 (25°–32.5°N, 75°–90°E)
EA	V850 (20°–45°N, 110°–130°E)
WNP	U850 (5°–15°N, 100°–130°E) minus U850 (20°–35°N, 110°–140°E)
NAM	U850 (5°–15°N, 120°–80°W) minus U850 (20°–30°N, 110°–80°W)
SAF	U700 (5°–15°S, 10°–30°E) minus U700 (22.5°–30°S, 15°–35°E)
AUS	U850 (0°–15°S, 90°–130°E) minus U850 (20°–30°S, 100°–140°E)
SAM	U850 (5°–15°S, 70°–40°W) minus U850 (22.5°–30°S, 60°–40°W)

SHLM and three regional monsoon (SAF, AUS, SAM) circulation index. The dashed lines indicate the linear trends. SHLM is canulated by the averaged of the three regional monsoon indices.

Part 4: CMIP6 simulation

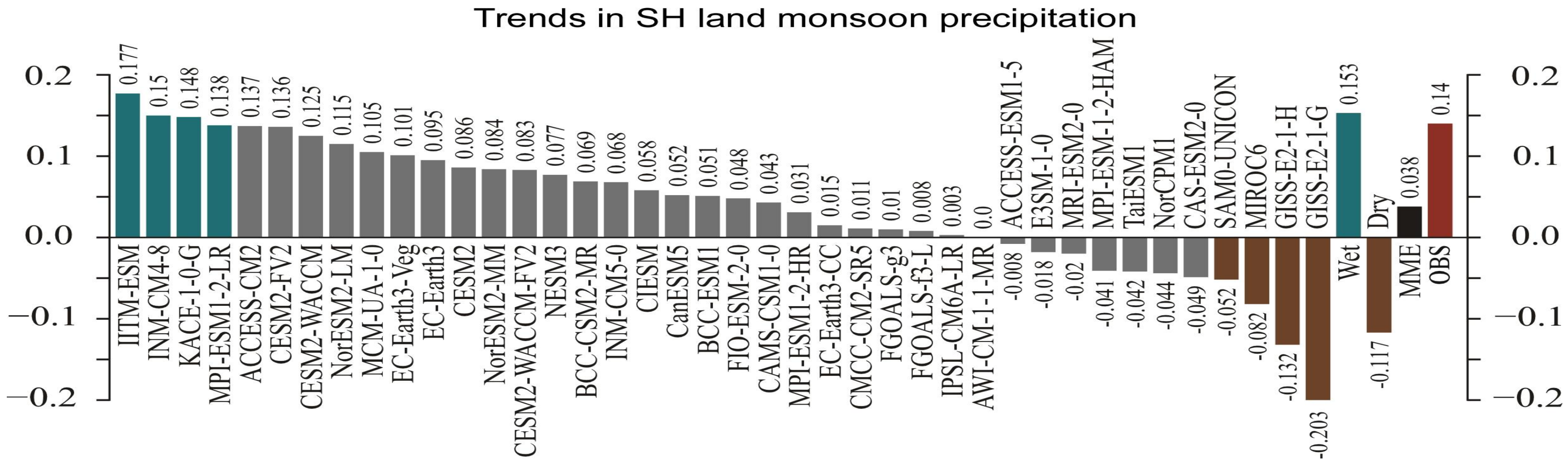

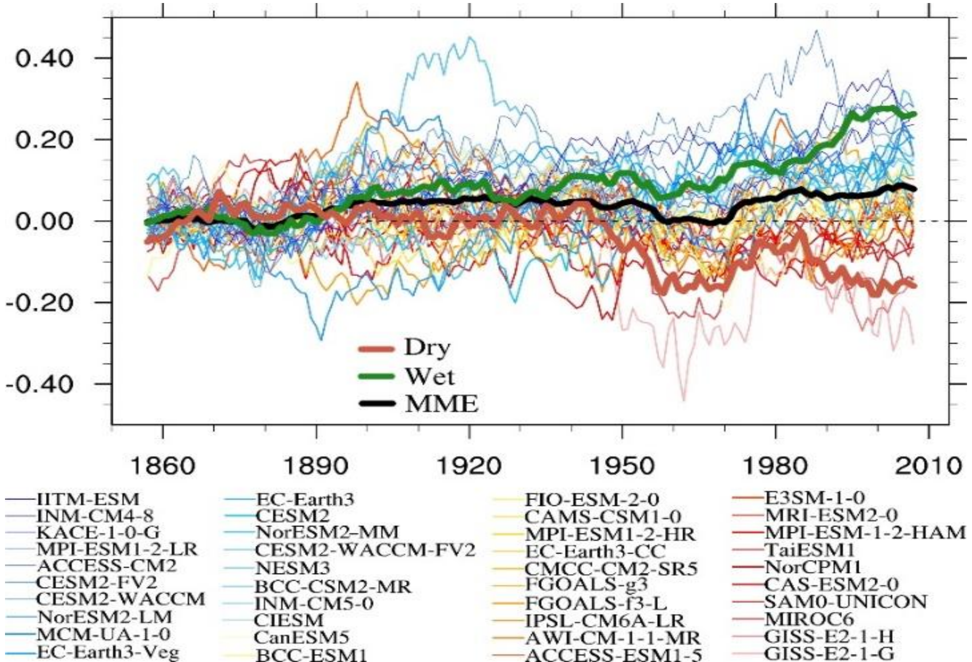

Evolution of SHLMP anomalous in 40 CMIP6 models relative to 1850-1879. Thin lines show the 15-year running mean of SHLMP in the individual model. The thick brown and green lines indicate the ensemble mean of four models with the largest dry and wet linear trends during 1850-2014, respectively. The thick black line denotes the 40-model ensemble mean.

Part 4: CMIP6 simulation

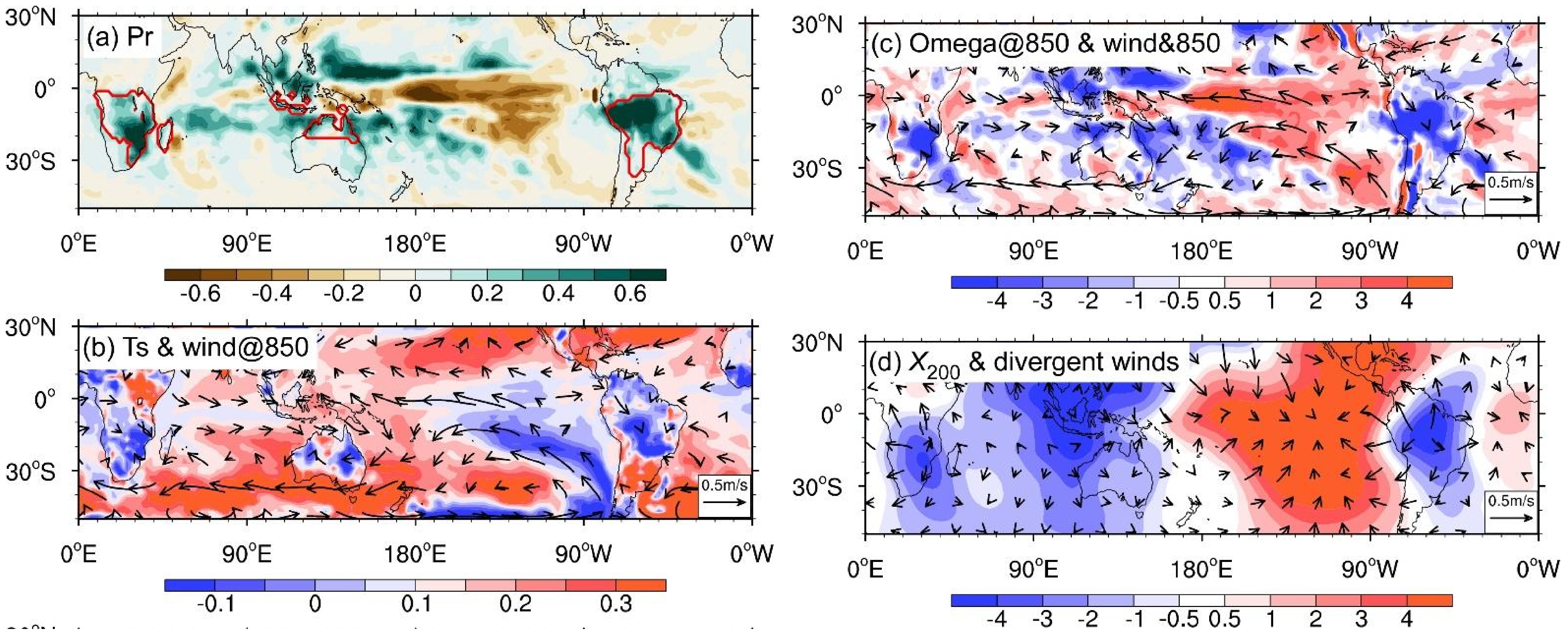

Figure 8 Difference in linear trends between the wet and dry models during 1850-2014. (a) for precipitation (mm d^{-1} $cent^{-1}$), (b) for surface temperature (shading, K $cent^{-1}$) and 850 hPa circulation (m s^{-1} $cent^{-1}$), (c) for 500 hPa vertical pressure velocity (shading, 100*omega, Pa s^{-1} $cent^{-1}$) and 850hPa circulation (m s^{-1} $cent^{-1}$), and (d) velocity potential (shading, 10^5 m^2 s^{-1} $cent^{-1}$) and divergence winds (m s^{-1} $cent^{-1}$) at 200 hPa.

Part 4: CMIP6 simulation

南京信息工程大学
Nanjing University of Information Science & Technology

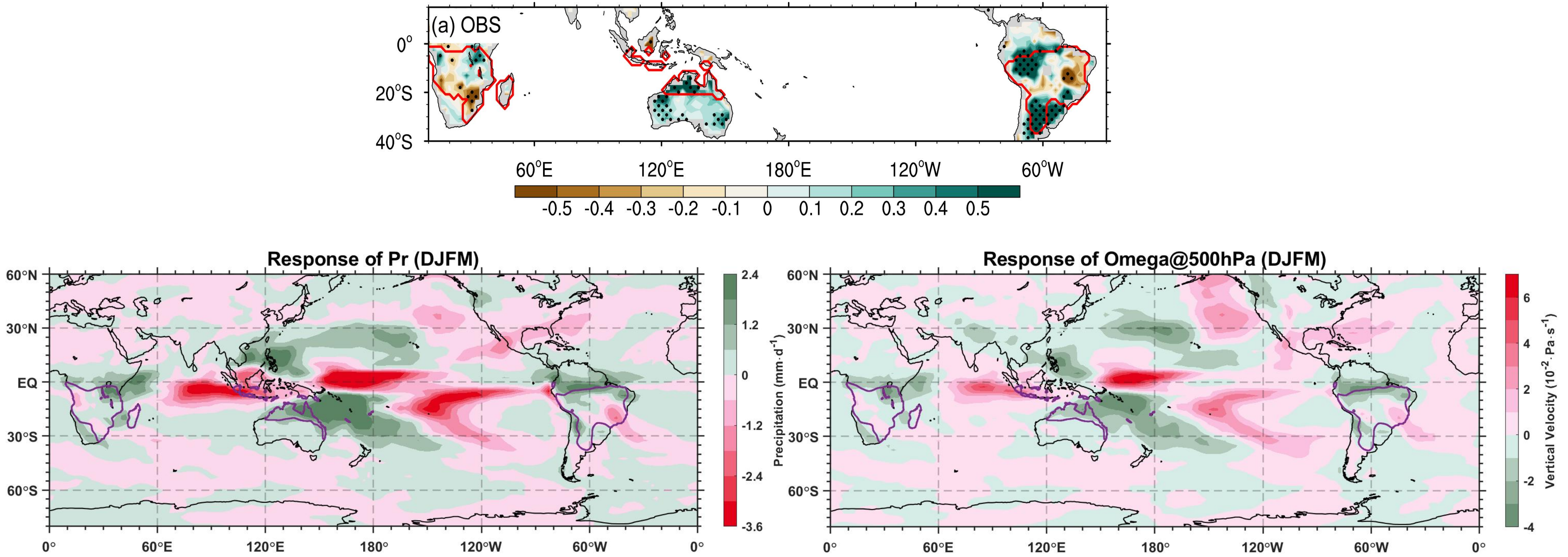

Figure 8 Difference in linear trends between the wet and dry models during 1850-2014. (a) for precipitation (mm d^{-1} $cent^{-1}$), (b) for surface temperature (shading, K $cent^{-1}$) and 850 hPa circulation (m s^{-1} $cent^{-1}$), (c) for 500 hPa vertical pressure velocity (shading, 100*omega, Pa s^{-1} $cent^{-1}$) and 850hPa circulation (m s^{-1} $cent^{-1}$), and (d) velocity potential (shading, 10^5 m^2 s^{-1} $cent^{-1}$) and divergence winds (m s^{-1} $cent^{-1}$) at 200 hPa.

Part 4: CMIP6 simulation

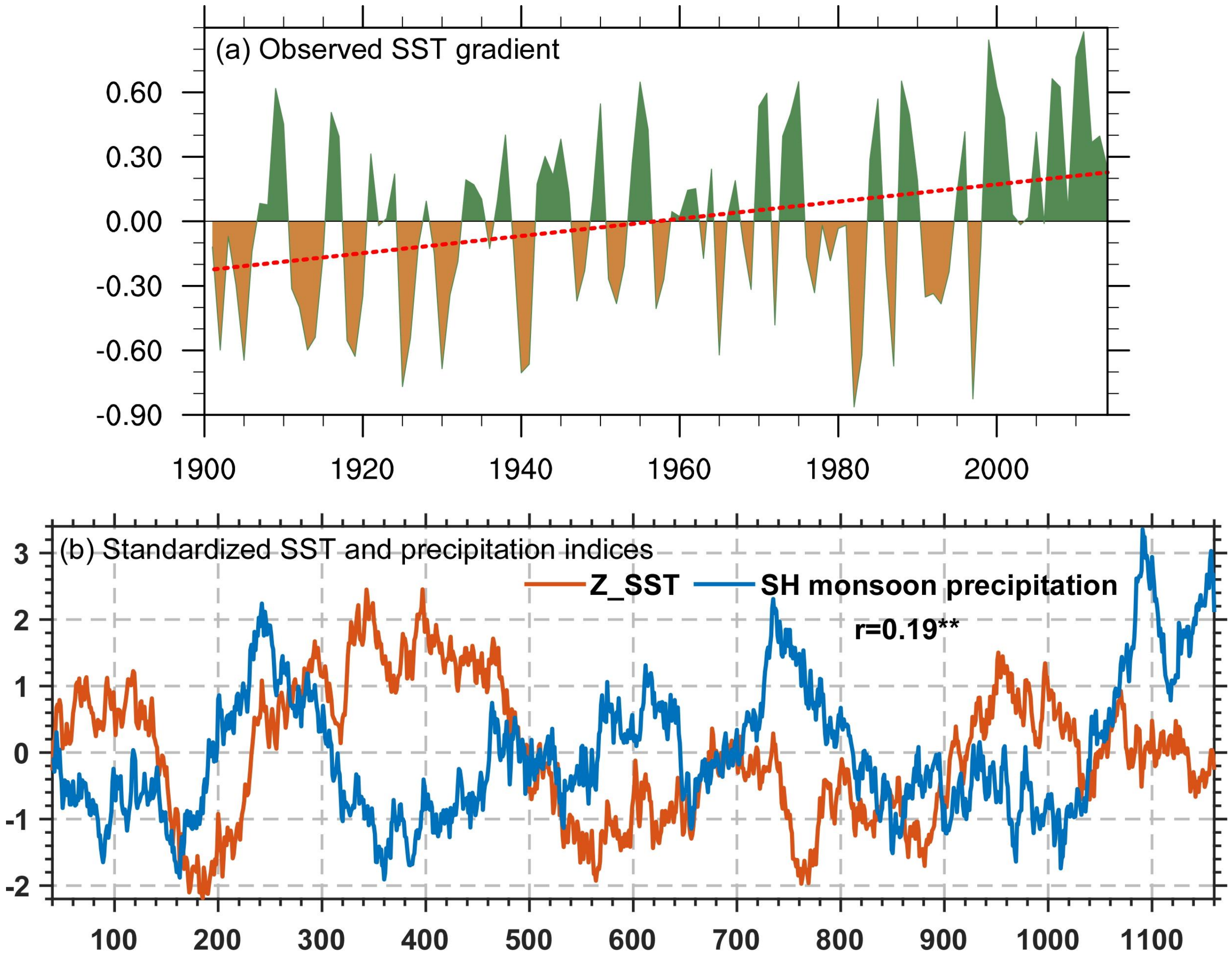

Figure 10 (a) Observed zonal SST gradient (Indo-Pacific region minus eastern Pacific region) index relative to the average of 1901-2014. (b) Standardized zonal SST gradient index and SH monsoon precipitation index after 79-y running mean in CESM2 preindustrial simulation. ** indicates significance at a 99% confidence level.

Part 4: Monsoon Vs. Hadley circulation

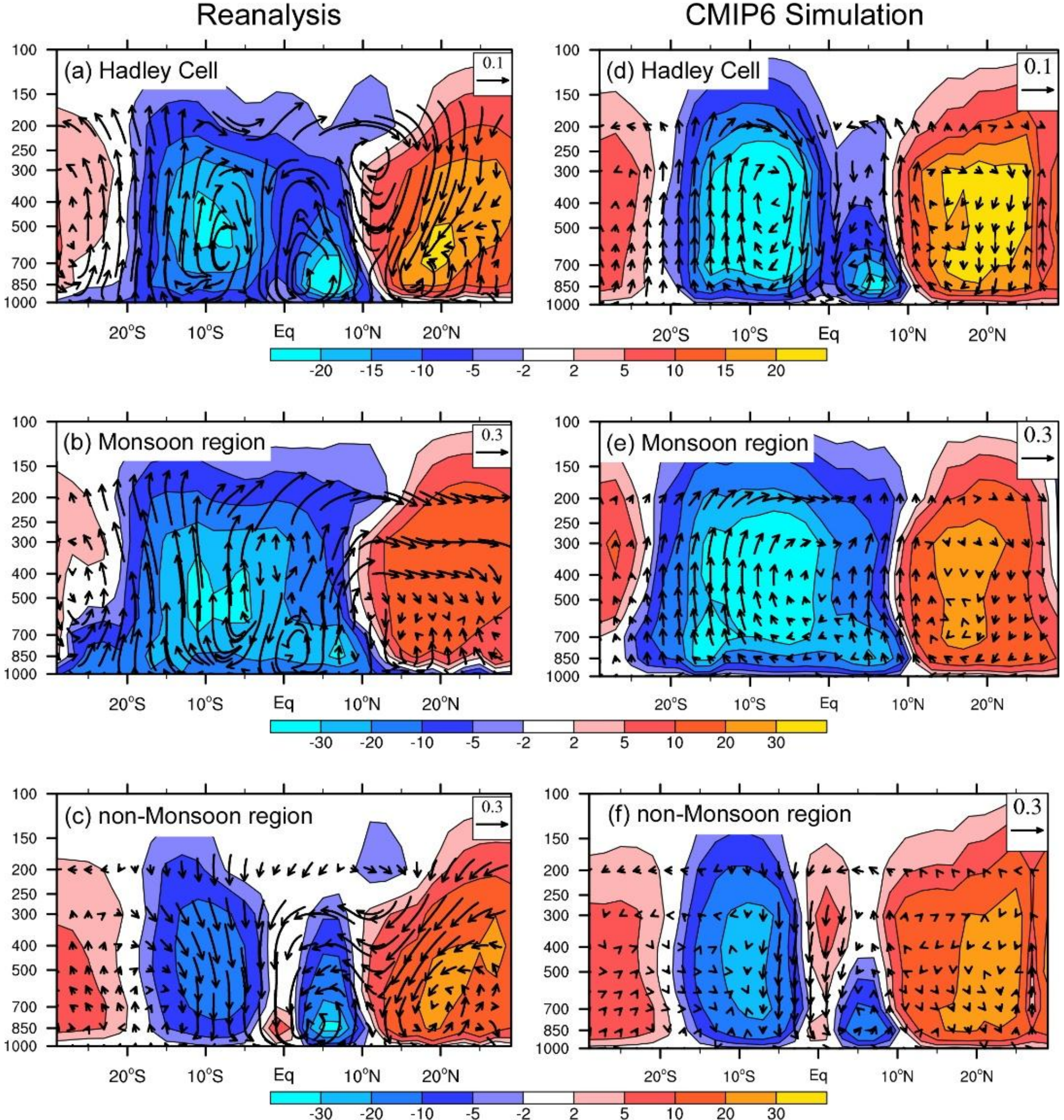

Climatology (shading) and linear trends of meridional divergence circulation from (left) NOAA-20C reanalysis and (right) CMIP6 models. (a) Zonal averaged Hadley circulation. (b) as (a), except for the monsoon region (10°E-50°E, 110°E-150°E, and 80°W-40°W). (c) as (a), except for the non-monsoon region. (d-f) as (a-c), except for the difference between wet and dry models. Shading shows the climatological mean of vertical pressure velocity (hPa d^{-1}). Vector is the composite of 100 times vertical velocity change (Pa s^{-1} $cent^{-1}$) with zonal and meridional wind trends (m s^{-1} $cent^{-1}$) in (a) and (b), respectively.

Part 5: Summary

南京信息工程大学
Nanjing University of Information Science & Technology

Observational datasets show the decrease in NH land monsoon during 1900-2014, and the SH land monsoon precipiation is increased during the same period. CMIP6 models well reproduced the decrease in NH monsoons, with the single forcing experiment demostrating the dominate role of external forcing. However, CMIP6 model underestimates the observed SH land monsoon trend. Analysis pointed to the zonal SST graident drives the SH monsoon increase since preindustrial.

✓ **What is the relative role of AA and GHG forcing in the centennial-scale NHLM precipitation trend?**

A: AA dominates the decline of NHLM precipitation, and GHG explains the GMST increase. AA is five time as the GHG on NHLM precipitation change, in terms of per GMST change.

✓ **Why does the AA forcing dominate the declining NHLM precipitation?**

A: AA's AOD decreases the surface irradiance for evaporation and more effectively alter the surface temperature gradients, thus monsoon circulation.

✓ **Which mechanism is responsible for the increase of SH monsoon?**

A: (i) The tropical zonal SST graident drives the Walker circulation change, which redistribute moisutre from the tropical ocean to the monsoon region. This SST graident may not full caused by the anthropogenic forcing. The nature varibility is one of possiblity.

(II) Regional Hadley circulation over the monsoon region dominates the zonal mean Hadley cell and ITCZ

Thanks for your attention!

Comments and suggestions are welcome!

jianc@nuist.edu.cn